[American Journal of Science, Vol. 311, May, 2011, P. 369–403, DOI 10.2475/05.2011.01]

American Journal of Science

MAY 2011

MODELING THE EVOLUTIONARY RISE OF ECTOMYCORRHIZA ON SUB-SURFACE WEATHERING ENVIRONMENTS AND THE GEOCHEMICAL CARBON CYCLE

LYLA TAYLOR*,†, STEVE BANWART**, JONATHAN LEAKE*, and DAVID J. BEERLING*

ABSTRACT. For the past two decades, the spread of angiosperm plants in the Cretaceous and Paleogene has been thought to have enhanced silicate weathering fluxes of Ca and Mg to the oceans, thereby drawing down atmospheric CO_2 and ultimately sequestering it in marine carbonate sediments. However, the rise of angiosperm trees in the Cretaceous was coincident with the evolution of ectomycorrhizal fungal associations in angiosperm and gymnosperm trees that have increasingly supplanted trees with the ancestral arbuscular-mycorrhizal associations. This represents the most profound alteration in root functioning to occur in plant evolutionary history, with far-reaching implications for weathering and soil biogeochemistry because the fine roots are enveloped with a fungal sheath. Ectomycorrhizal fungi provide the main nutrient and water-absorbing interface with soil, and the pathway through which organic acids and protons are actively secreted at the scale of individual mineral grains. Here, we test the hypothesis that the rise of ectomycorrhizal trees was a major contributor to the drawdown of atmospheric CO_2 over the past 120 Ma through enhanced silicate weathering. We developed a process-based soil chemistry model incorporating the effects of plants with ancestral arbuscular mycorrhizas, and more recently evolved ectomycorrhizas on soil chemistry via its effects on the biological proton cycle, and integrated it into a leading model of the long-term carbon cycle (GEOCARBSULF). Our mechanistic, process-based modeling reveals that the rise of ectomycorrhizal trees can explain the CO_2 drawdown previously attributed empirically to the spread of angiosperms. We suggest, therefore, that the evolutionary rise of ectomycorrhizas represents an important driving force of the long-term carbon cycle by enhancing chemical weathering and draw-down of atmospheric CO_2 into marine carbonates.

Key words: Long-term carbon cycle, biological weathering, fungal weathering

INTRODUCTION

On multi-million-year timescales, the release of calcium and magnesium during the weathering of continental silicate minerals is considered to be a controlling factor regulating the long-term carbon cycle, atmospheric CO_2 and, therefore, global climate. The overall process can be represented by the following expression which summarizes many intermediate steps (Ebelmen, 1845; Urey, 1952; Berner and Maasch, 1996):

$$CO_2(air) + CaSiO_3(land) \rightarrow SiO_2(land, sea) + CaCO_3(sea) \quad (1)$$

* Department of Animal and Plant Sciences, University of Sheffield, Sheffield S10 2TN, United Kingdom
** Kroto Research Institute, North Campus, University of Sheffield, Sheffield S3 7HQ, United Kingdom
† Corresponding author: L.L.Taylor@sheffield.ac.uk

A similar, but more complicated expression holds for magnesium, which substitutes for calcium on the ocean floor and results in the deposition of calcium carbonate (Hardie, 1996).

Plant activities enhance the weathering of terrestrial silicate rocks by several mechanisms, including: i) the alteration of soil solution chemistry by ion exchange during nutrient uptake, respiration, and organic matter decomposition, ii) changes to soil hydrology as a result of evapotranspiration, and iii) physical binding and stabilization of soil particles (Berner and others, 2003). Such mechanisms are represented by empirical functions in models of the geochemical carbon cycle that lump all processes into a single effect (Berner, 1991, 1994; Berner and Kothavala, 2001; Bergman and others, 2004; Berner, 2006a, 2006b, 2008). These empirical functions attempt to represent differences in the weathering efficiencies of vegetation as a result of evolutionary innovations, such as the origination and geographical spread of trees in the Palaeozoic, and the later rise of angiosperms in the Mesozoic. For the Palaeozoic, these functions are based on contemporary field studies measuring the differences in stream-water concentrations of calcium and magnesium as influenced by trees or by lichens and mosses (Drever and Zobrist, 1992; Arthur and Fahey, 1993; Moulton and others, 2000). Comparing these studies, Berner (2004) showed that trees increase Ca and Mg concentrations by a factor of four compared to lichens and mosses.

In the 1980s, several authors suggested that the spread of angiosperms, especially deciduous angiosperms, might have accelerated silicate weathering (Knoll and James, 1987; Volk, 1989), due to differences in nutrient cycling between deciduous and evergreen trees. A 114 percent increase in Ca and Mg delivery to the oceans during the major angiosperm radiation approximately 130 to 80 Ma (Crane and Lidgard, 1989) was supported by comparison of independent proxy data (Ekart and others, 1999) with GEOCARB III (Berner and Kothavala, 2001). However, subsequent field-based observational evidence for differences in weathering efficiency between angiosperm and gymnosperm vegetation is equivocal (Berner and others, 2003; Taylor and others, 2009). Furthermore, important gymnospermous trees of the Permian, Mesozoic and Paleogene were deciduous (Douglas and Williams, 1982; Spicer and Parrish, 1986; Spicer and Chapman, 1990; Rees and others, 1999; Falcon-Lang, 2000), and many tropical angiosperms are evergreen, so the deciduous leaf habit cannot be considered a purely angiosperm trait.

Based on an extensive synthesis of the literature, we recently developed an alternative hypothesis. We pointed out that an overlooked and potentially important biological factor driving atmospheric CO_2 change during the Mesozoic and Cenozoic is the rise of a major group of symbiotic soil fungi forming ectomycorrhizas with tree roots (Taylor and others, 2009). Our review presented evidence that ectomycorrhizal (EM) fungi differ from the ancestral arbuscular mycorrhizal (AM) fungi in that they exude low molecular weight organic chelators (for example, Griffiths and others, 1994; Sun and others, 1999; van Hees and others, 2006; Gadd, 2007), and may acidify soils to a greater extent (for example, Cromack and others, 1979; Sohet and others, 1988; Binkley and Valentine, 1991; Augusto and others, 2002). EM fungi prevent direct contact between soil and infected root tips, whereas AM fungi do not (fig. 1). EM fungi associate with both eudicot angiosperms and gymnosperms, including locally to regionally dominant boreal, tropical, and temperate tree families such as Pinaceae, Dipterocarpaceae, and Fagaceae. We therefore postulated that the origination and spread of EM fungi that occurred over the same interval as the rise in angiosperms represents an important contributory biotic factor driving the drawdown in atmospheric CO_2 over the past 120 million years.

Here, we report the development of a process-based model that accounts for the differing effects on soil chemistry of fine roots, AM and EM fungi to address this biotic

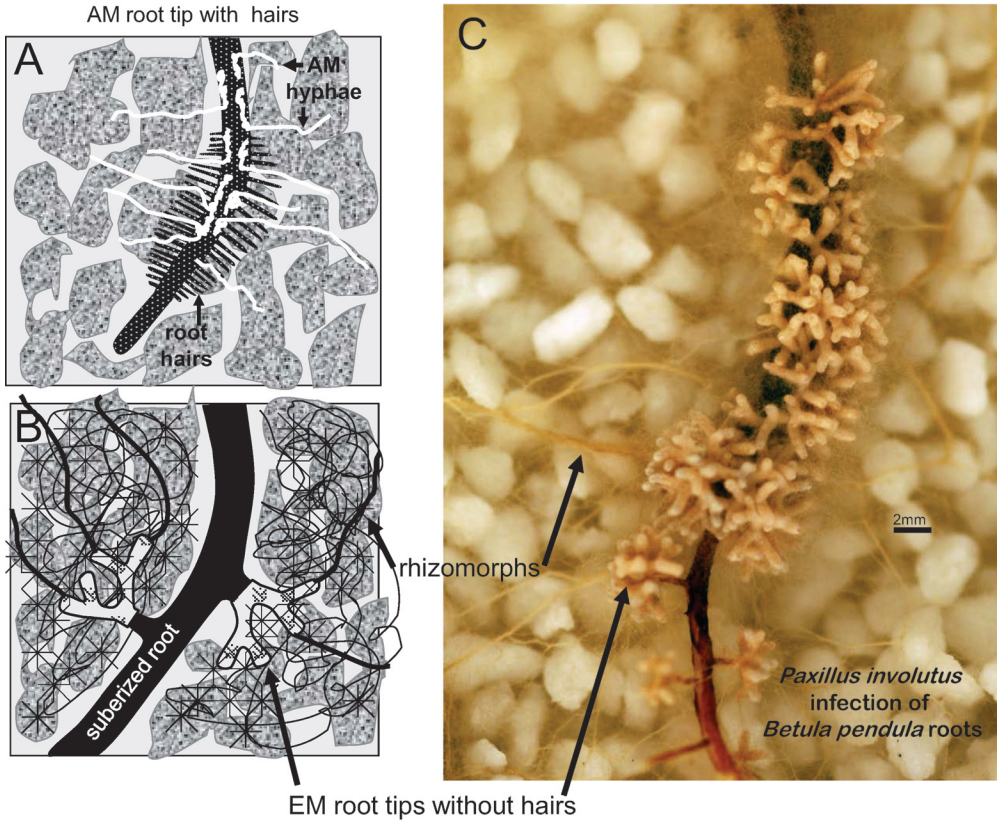

Fig. 1. Roots and mycorrhizal fungi. Arbuscular-mycorrhizal (AM) roots, in particular the root hairs, exchange ions with the surrounding medium (A). Their capacity for nutrient uptake is enhanced but not superseded by AM fungi. Ectomycorrhizal (EM) fungi fundamentally alter plant-mineral relationships by preventing direct contact between soil and colonized root tips (B, C). EM root tips are sheathed with mycelium and have no active root hairs. Since EM fungi are almost solely responsible for nutrient uptake for the host tree, they have much longer hyphal lengths than AM fungi. Cordlike bundles of hyphae (rhizomorphs) transport nutrients from the most distant hyphae to the roots. Photo: Adele Duran and Jonathan Leake.

weathering hypothesis. Our model includes representation of the biological cycling of protons and alkalinity (Banwart and others, 2009) occurring in discrete regolith zones: i) the soil which is in contact with or under the influence of living roots and mycorrhizal hyphae (the *mycorrhizosphere*), and ii) the remaining *bulk soil* where abiotic weathering dominates. We developed numerical routines for calculating weathering rates on basalt and granite that incorporate simple yet rigorous equilibrium chemistry (Stumm and Morgan, 1996) and rate laws (Palandri and Kharaka, 2004; Brantley, 2008), and implemented these in a version of the GEOCARBSULF model (Berner, 2006b, 2008) to mechanistically evaluate the above hypothesis. In the mycorrhizosphere, weathering is largely driven by ion exchange during nutrient uptake, and the exudation of organic acids. Our model also reflects the differing abilities of the two types of mycorrhizal fungi and roots to direct nutrient uptake activity to nutrient sources such as Ca and Mg bearing minerals in the mycorrhizosphere.

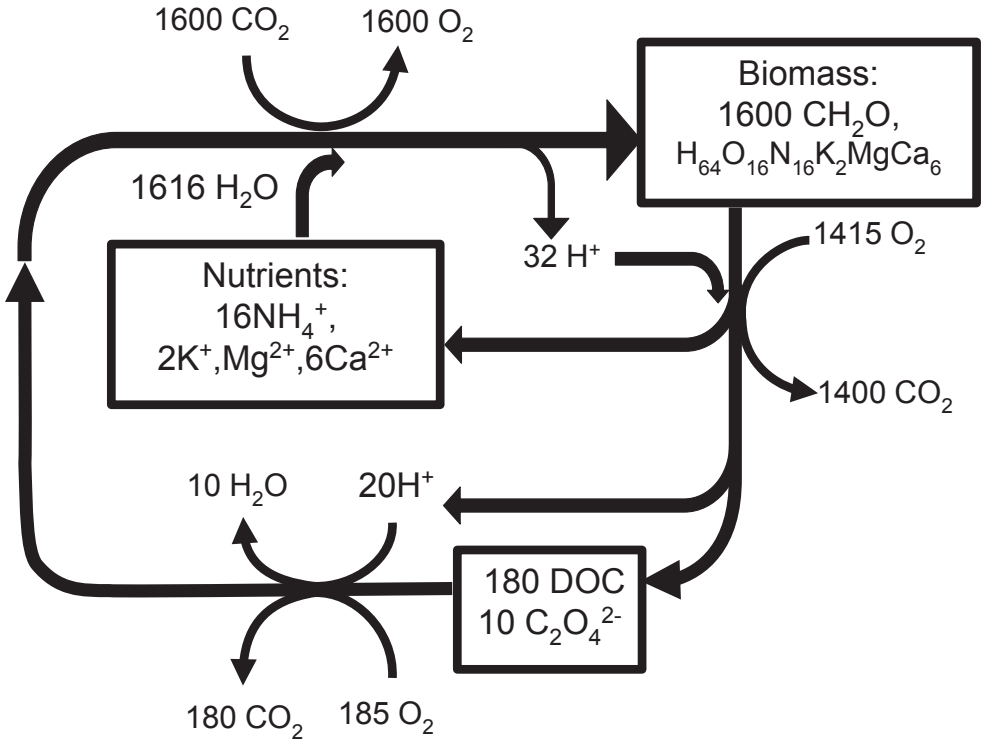

Fig. 2. The biological proton cycle. This figure shows the stoichiometry used by Banwart and others (2009) in their model of weathering processes in the Risfallet catchment, Sweden, in the idealized case where no ions enter or leave the system. It assumes that the reactive fraction of the dissolved organic carbon (DOC) can be modeled as oxalate.

THE BIOLOGICAL PROTON CYCLE

The effects of both tree roots and mycorrhizal fungi on sub-surface weathering environments can be unified through the concept of the biological proton cycle (Banwart and others, 2009, fig. 2). The biological proton cycle describes the stoichiometry of reactions during the uptake of mineral nutrients by plants and symbiotic root fungi during growth and the subsequent return of these nutrients during decomposition of organic matter. Overall, these reactions determine the net flux of protons into and out of the sub-surface environment and therefore the acid-base balance and its influence on the pH of the mineral weathering environment (fig. 2).

Nutrient Uptake During Plant Growth

The biological proton cycle is initiated when fine roots and fungal hyphae expel protons into the surrounding medium, thereby attracting nutrient cations into the cells against their concentration gradients. This process acidifies the solution in the immediate vicinity of these structures. Nutrient anions, on the other hand, may be imported into the cell together with charge-balancing protons (Marschner, 1995), alkalizing the surrounding solution. Uptake can lead to alkalization or acidification depending on the nitrogen form available (NO_3^- or NH_4^+, respectively). Release of organic anions can also have variable effects on pH.

Organic Acid Exudation

Unlike AM fungi, EM fungi exude low molecular weight organic acids (LMWOAs). Oxalate is one of the most important LMWOAs exuded by EM fungi (Landeweert and others, 2001; Hoffland and others, 2004), under both field (Cromack and others, 1977; Cromack and others, 1979) and laboratory (van Hees and others, 2006; Johansson and others, 2008) conditions. Oxalate production by EM fungi varies with a variety of factors including hyphal density, fungal species, and the minerals present (Griffiths and others, 1994; Arvieu and others, 2003; Casarin and others, 2003; Rosling and others, 2004; van Hees and others, 2006). Arvieu and others (2003) and Casarin and others (2003) observed lower hyphosphere pH with exudation of oxalate for EM fungi where the external reference pH was above the pK values of the ionization constant for oxalate. LMWOAs have a residence time in the soil solution on the order of hours (van Hees and others, 2005a), and although this can be longer in the mineral soil than in the organic layer due to adsorption to the solid phase, these authors suggested that LMWOAs turn over in solution up to 80 times per day.

Decomposition

Plant material provides a terrestrial reservoir of alkalinity and base cations such as Ca^{2+}, Mg^{2+}, and K^{+}, which are returned to the soil during decomposition (fig. 2), stemflow and foliar leaching. A second pool of more slowly decomposing transportable material sequesters alkalinity from the soil profile, resulting in net acidification (Banwart and others, 2009). In a theoretical steady-state forest, where decomposition keeps pace with growth, and without loss of cations or organic matter from the system, there should be no net acidification of the soil. Net acidification occurs in aggrading ecosystems (Nilsson and others, 1982; Knoepp and Swank, 1994; Hüttl and Schaaf, 1995; Jobbágy and Jackson, 2003) where uptake during canopy development exceeds return of nutrients in litter (Miller, 1995), and in harvested and natural systems where biomass is removed and nutrients are not returned to the soil. Bolan and Hedley (2003) reviewed the evidence for acidification of agricultural soils due to disruption of the C, N and S cycles via removal of plant material, accumulation of partially-decomposed organic matter, and nutrient leaching. Nutrient loss is also accelerated by rainfall following forest fires (Malmer, 1996), as well as by leaching and volatilization (Boerner, 1982). Reactive organic anions associated with the slowly decomposing pool of organic matter may act as ligands, contributing to the weathering of minerals. We followed Banwart and others (2009) in modeling these reactive species as oxalate.

MODELING APPROACH

Our approach to modeling the effects of the arbuscular and ectomycorrhizal fungi on Ca-Mg silicate mineral weathering and atmospheric CO_2 aims to capture the key processes underpinning the biological proton cycle (fig. 2) with a soil module that can be implemented within an established geochemical carbon cycle model (Berner, 2006b, 2008).

Under the assumption that the largest fluxes of Ca and Mg will come from that part of the global regolith undergoing far-from-equilibrium weathering on young reactive mineral soils with low clay content, we restrict our attention to the vadose zone (above the water table). We divide the vadose zone into the bulk soil solution and the soil that is under the influence of fine roots and mycorrhizal hyphae (the mycorrhizosphere).

Using the conceptual model shown in figure 2, and expressing respiration as a function of net primary productivity (NPP), we can link the pH of both the mycorrhizosphere and bulk soil, and the concentration of organic ligands in the bulk soil, directly to carbon fixation in the form of NPP.

Combined with the volumes of the bulk soil and mycorrhizosphere, the mineralogy of the parent materials, and parameters already calculated by GEOCARBSULF, we calculate fluxes of Ca and Mg to the oceans at one million year timesteps throughout the last 200 Ma. This timespan encompasses the evolution and spread of both angiosperms and the ectomycorrhizal symbiosis.

Terrestrial Net Primary Productivity (NPP)

The primary driving force for the biological proton cycle is the NPP of terrestrial vegetation because it ultimately provides the carbon energy flux into roots and mycorrhiza that take up mineral nutrients and drive weathering in the sub-surface environment (fig. 2). Our model therefore begins by estimating the changing global terrestrial NPP over the Phanerozoic based on Michaelis-Menten-type functions employed in previous geochemical models (Berner and Kothavala, 2001; Bergman and others, 2004; Berner, 2006a). These functions approximate changes in the rate of photosynthesis due to the effects of varying temperature and the relative concentrations of CO_2 and O_2 in the atmosphere in the efficiency of Rubisco, the primary carboxylating enzyme in C_3 land plants.

We evaluated these functions by comparing them with independent estimates of global terrestrial NPP from simulations in which a process-based terrestrial carbon cycle model is forced with palaeoclimate simulations for six different internals over the Phanerozoic (Beerling and Woodward, 2001) (fig. 3A). Of the four functions shown, the fire-corrected function of Bergman and others (2004) best fits the six NPP estimates. This is the most complicated of the four functions tested (see their eqs 3-8), and the only one that successfully fits the Carboniferous estimate. All four functions were scaled using a smoothed version of the land plant colonization function of Bergman and others (2004) in the Palaeozoic, and a modern NPP of 62 GtC y^{-1} (Saugier and others, 2001).

Results from free-air CO_2 enrichment (FACE) experiments with different ecosystems provide a means of testing the CO_2-responses of the NPP functions (Norby and others, 2005). FACE data include the responses of one EM tree (*Pinus taeda*), one AM tree (*Liquidambar styraciflua*), and several species of *Populus* which may be AM or EM. All four of our test NPP functions fit the FACE data well (fig. 3B). However, FACE experiments exposed ecosystems to a CO_2 level that is only about twice that of the present day, whereas atmospheric CO_2 may have been half an order of magnitude higher than the pre-industrial present during the Cretaceous.

Distribution of Roots and Hyphae in Soil

We modeled the distribution of fine roots and EM hyphae in soils using fine root data (Thelin and others, 2002) and hyphal data (Wallander and others, 2004) from Jämjö, Sweden. Wallander and others (2004) measured the biomass of mycelium in both soil and in sand in-growth bags, and hyphal lengths in the in-growth bags, allowing soil biomass data to be converted to hyphal lengths in soil under the assumption that hyphal diameter and mass per unit length, but not total length, are the same for sand and for soil. With these data, we can check whether EM fungi and fine roots have similar distributions with soil depth. Comparable data are lacking for AM trees. Since AM hyphae colonize AM root systems evenly with depth for three of the four trees examined by Ingleby and others (1997), we assume that AM hyphal lengths have a similar depth distribution to AM fine root lengths.

Following Cerling (1991), we used an exponential soil CO_2 production function:

$$\phi(z) = \phi(0)\exp(-z/\bar{z}) \quad (2)$$

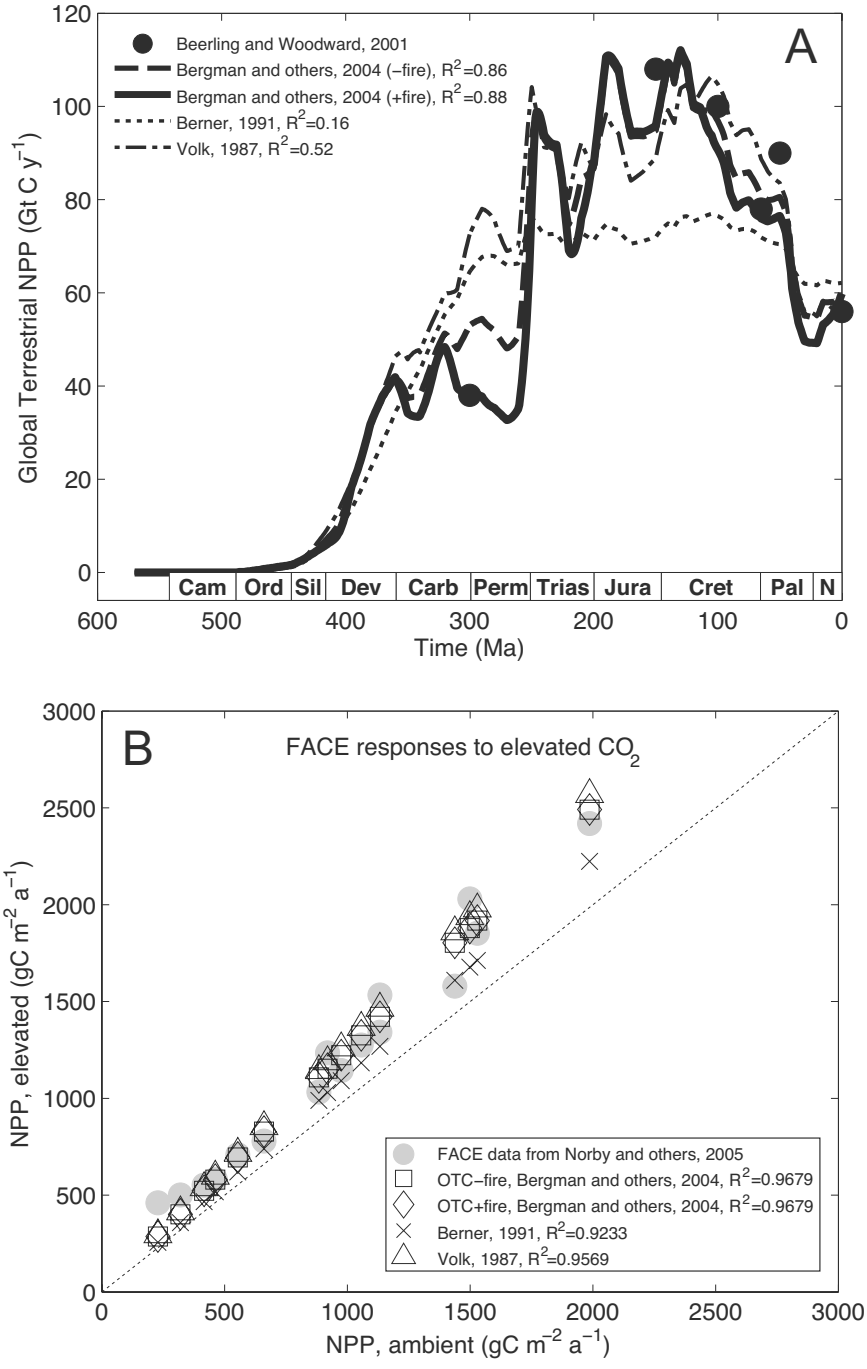

Fig. 3. Response of vegetation to changes in atmospheric CO_2. (A) Terrestrial net primary productivity (NPP) throughout the Phanerozoic. Approaches used in long-term carbon cycle models are based on various Michaelis-Menten formulations (Volk, 1987; Berner, 1991; Bergman and others, 2004) and these have been scaled using a smoothed version of the plant colonization function of Bergman and others (2004) and modern-day NPP (Saugier and others, 2001). Estimates of NPP from the vegetation model of Beerling and Woodward (2001) are included for comparison. (B) Response of NPP to elevated CO_2.

where $\bar{z}$ is a characteristic depth which, when multiplied by the fine root or hyphal length density $\phi(0)$ at the top of the soil (depth z=0), gives the integral of the production function, that is, the total length of fine roots or hyphae, over all depths. We expect equation (2) to describe the distribution of respiring organisms with depth, and therefore also the lengths of fine roots and mycorrhizal hyphae and the soil volume containing them.

The fits for *Picea abies* are good for both fine roots (fig. 4A) and EM hyphae (fig. 4B) in the mineral soil. There are fewer fine roots in the organic layer than our simple function predicts, but a more complicated distribution, such as Gaussian, does not fit the data in the mineral soil as well as the exponential fit to all data in the mineral soil only (fig. 4A).

Equation (2) fits the hyphal data for *Picea abies* very well, even in the organic layer (fig. 4B). High hyphal lengths near the surface allow *Picea abies* to take advantage of the organic nitrogen in the organic layer. Unfortunately, similar data are lacking for other trees. There are mixed *Quercus-Picea* stands at Jämjö, where the distribution of hyphae is dominated by *Picea abies* in the organic layer, with hyphal lengths that exceed those of the pure *Picea abies* stands. This is probably due to partitioning of the soil between the two species as a result of competition, as suggested by Wallander and others (2004). Therefore, in the mineral soil, the dominant hyphae may be associated with *Quercus robur*. If we ignore the data from the organic layer and extrapolate the remaining data to the top of the soil, we get a hyphal length density of 125 m cm^{-3} (soil) for *Quercus robur*.

We assume that there is little organic material in the soils of interest for global weathering, and therefore we ignore both the lack of fine roots and the extreme hyphal lengths in the organic layer of this Swedish forest and use the same for both fine roots and hyphae.

Jackson and others (1997) expressed the global distribution of fine roots in terms of an extinction function that is not identical to equation (2), but we can readily derive parameters for equation (2) with their data. If we use area-weighted means for temperate and tropical forests and plot the resulting characteristic depths for their woody biomes with NPP data from Saugier and others (2001), we get a linear relationship (fig. 5A):

$$\bar{z}(cm) = 10.1(cm) + 0.026 \times NPP\left(\frac{gC}{m^2 y}\right) \qquad (3)$$

Equation (3) allows us to eliminate the characteristic depth from our list of model parameters. We did not find any relationship between NPP and fine root lengths, either at the top of the soil ($\phi(0)$) or throughout the soil.

We can add the characteristic depths for the stands at Jämjö to figure 5A. Using the net productivities and wood densities from Thelin and others (2002), a conversion factor of 0.3879 gC g^{-1} DWT derived from the stoichiometry of Schnoor and Stumm (1986), and a factor of 1.65 to convert above-ground NPP to total NPP derived from data of Saugier and others (2001), we obtained a total NPP of 385 gC m^{-2}(land) y^{-1} for the *Picea abies* (spruce, S) stands and 345 gC m^{-2}(land) y^{-1} for the mixed (M) stands. Using these values, equation (3) predicts characteristic depths of 19 cm for mixed stands, which is close to those calculated from the actual distributions of hyphae (15.4 cm) and fine roots (18-23 cm, depending on whether the values in the E layer are averaged or not). We calculated characteristic depths of around 10 cm for both fine roots and hyphae in the spruce stands, which is shallow compared to that predicted by equation (3) (20 cm).

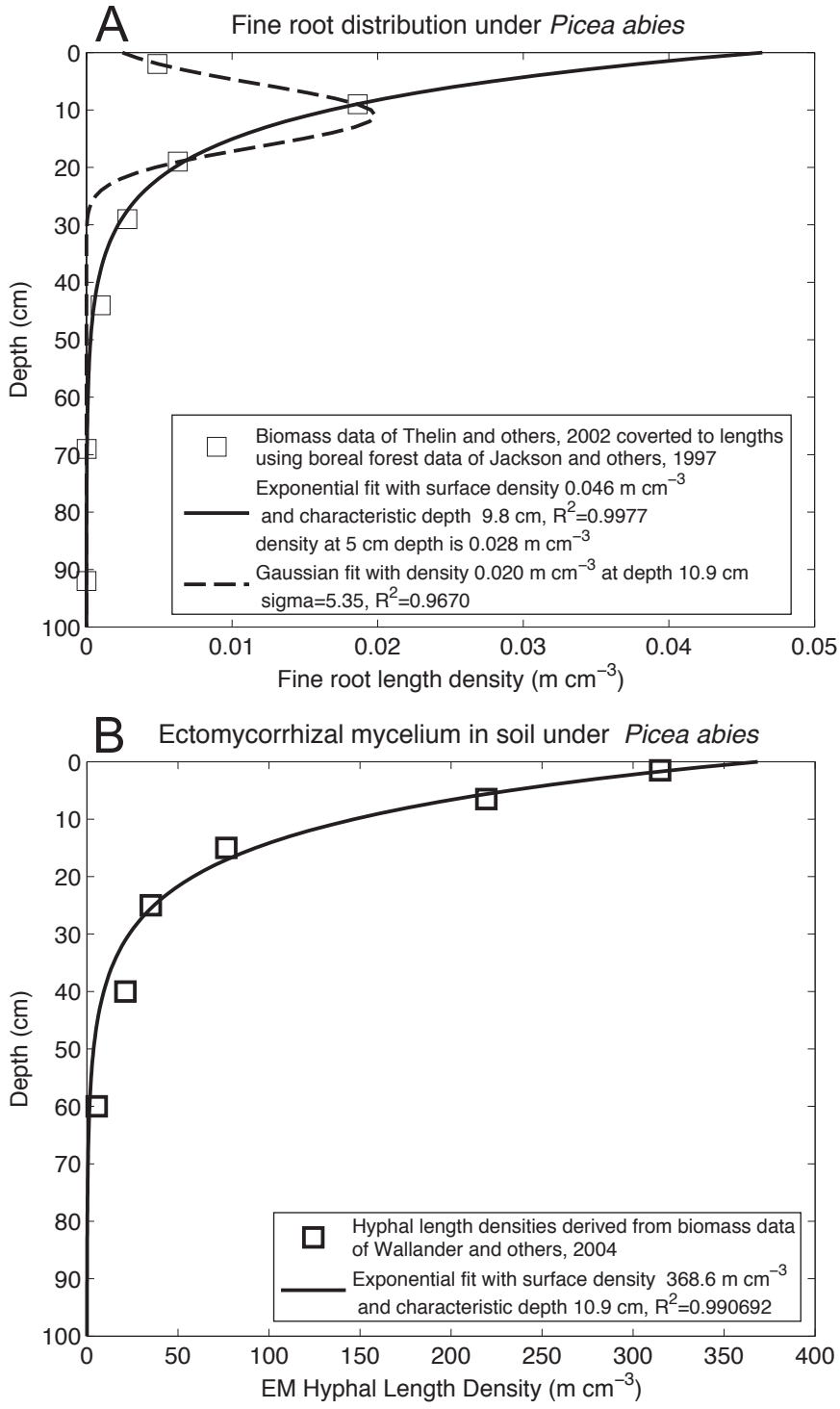

Fig. 4. (A) Fine root (Thelin and others, 2002) and (B) ectomycorrhizal hyphal (Wallander and others, 2004) distribution with depth at Jämjö, Sweden.

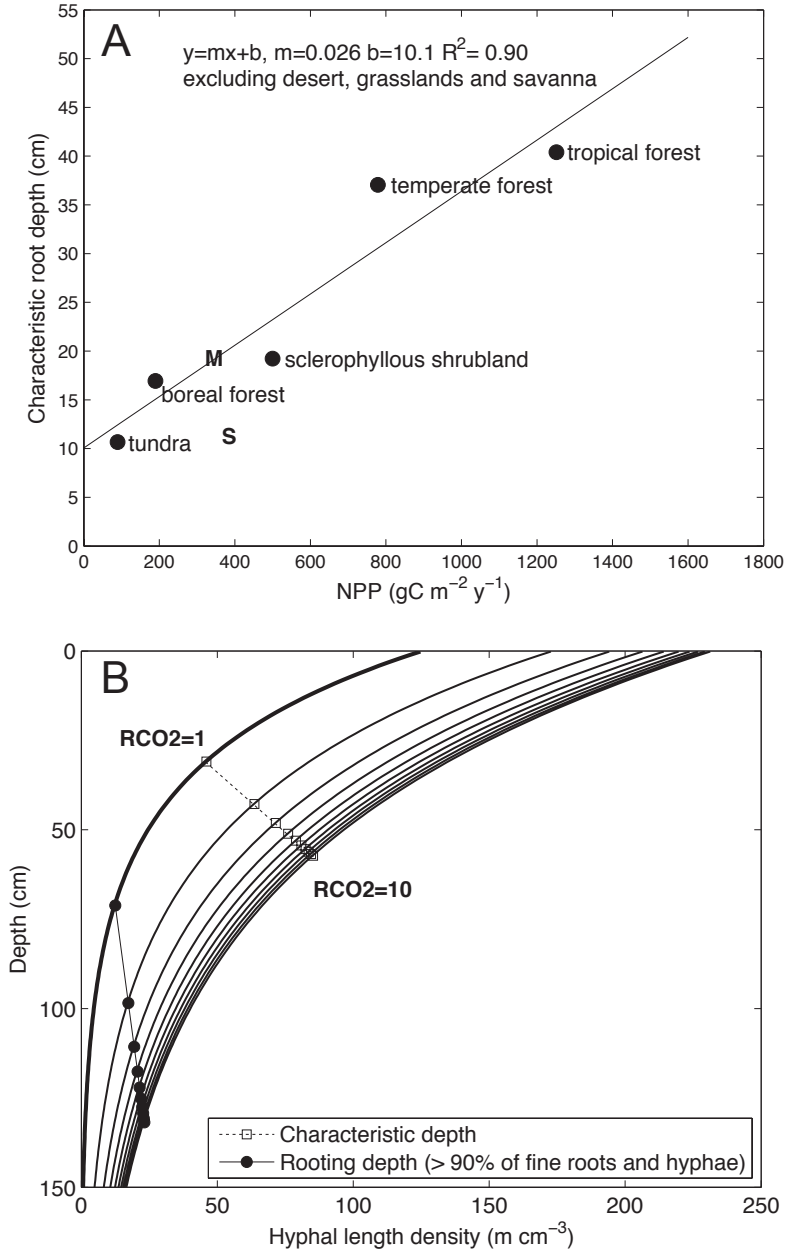

Fig. 5. (A) The characteristic depth describing the distribution of fine roots in soil is a linear function of net primary productivity (NPP). We converted the fine root distributions given by Jackson and others (1997) to characteristic depths using area-weighted means for depths in temperate and tropical forests. The NPP data are from Saugier and others (2001). M and S show data for the mixed (*Quercus-Picea*) and spruce (*Picea abies*) stands at Jämjö, Sweden, respectively, calculated from data published by Thelin and others (2002). (B) The depth distribution of ectomycorrhizal hyphae depends on RCO2, the ratio of atmospheric CO_2 at any time t to that of the preindustrial present. We started with a distribution defined by two parameters: a hypothetical modern hyphal length density at the top of the soil of 125 m cm^{-3} derived from the data of Wallander and others (2004) and a characteristic depth of 30 cm calculated using an NPP of 800 gC m^{-2} y^{-1} appropriate for temperate forests (Saugier and others, 2001) for RCO2=1. Then we applied equation (4) to get the hyphal length density and characteristic depth for $2 \leq RCO2 \leq 10$. Both the characteristic depth and a rooting depth, defined as that depth above which 90% of fine roots and hyphae are found, are marked on the curves.

Root and Hyphal Responses to Elevated CO_2

We define $R = \dfrac{\phi(elev)}{\phi(amb)}$ to be the fine root or hyphal response, and $P = \dfrac{plant(elev)}{plant(amb)}$ to be the response of the coarse roots and aboveground parts to elevated (twice ambient, linearly scaled as necessary) CO_2 as derived from the literature. These values give the response to a unit change in "RCO2", the ratio of CO_2 at time t to that at 0 Ma.

The change in NPP for an arbitrary RCO2 is RNPP, which is the ratio of our calculated NPP for time t and that for 0 Ma. $\phi_0(0)$ and $\phi_t(0)$ are the fine root or hyphal lengths at the top of the soil (z=0) at time 0 Ma and time t respectively. The equation

$$\phi_t(0) = \phi_0(0) \times \left(1 + \frac{R-1}{P-1}(RNPP - 1)\right) \tag{4}$$

satisfies the following conditions:

1. if RNPP = 1, then $\phi_t(0) = \phi_0(0)$
2. if RNPP = P, then $\phi_t(0) = \phi_0(0) \times R$
3. if RNPP $\leq$ 1, then $\phi_t(0) \leq \phi_0(0)$
4. if RNPP $\geq$ 1, then $\phi_t(0) \geq \phi_0(0)$

Equation (4) should also be used for the characteristic depth, instead of using equation (3) with the NPP for time t, because the latter may not reflect changes in root-shoot ratio. Instead, we use equation (3) to get $\bar{z}$ at 0 Ma and then apply equation (4) to get $\bar{z}$ at time t. The distribution of fine roots is known to shift downwards under elevated CO_2 (Norby and others, 2004), and although it is not clear what function describes this shift, our treatment of root responses captures this effect (fig. 5B).

Soil Respiration

Respiration is needed to calculate the partial pressure of CO_2 in the soil, because CO_2 affects the pH of the soil solution via the carbonate system (Stumm and Morgan, 1995). Malhi and others (1999) present data for tropical, temperate and boreal forests which allow us to infer a simple relationship between respiration and NPP. Dividing the sum of the values for below-ground heterotrophic and autotrophic respiration by NPP, we get a mean value of 1.5 $\times$ NPP for total respiration for the three forest types.

The diffusion equation describes CO_2 concentrations in soil:

$$\frac{\partial C_s}{\partial t} = D_{air}\varepsilon\rho\frac{\partial^2 C_s}{\partial z^2} + \phi(z) \tag{5}$$

where C_s is the concentration of CO_2 in soil, t is time, D_{air} is the diffusion constant for CO_2 in air, ε is the free-air porosity, ρ is tortuosity, z is depth, and $\phi(z)$ is a CO_2 production function for the soil, following the notation of Cerling (1991). As we used equation (2) for our production function as described above, our solution to equation (5) for CO_2 in soil is

$$C_s(z) = \frac{\phi(0)\bar{z}^2}{D_{air}\varepsilon\rho}(1 - \exp(-z/\bar{z})) + C_{air} \tag{6}$$

The Mycorrhizosphere

The exponential distribution of fine roots and hyphae defines a combined mycorrhizosphere, such that the organisms acidify the film of water on the minerals found there. We assume AM fungi are evenly distributed on the AM root system, with the fungi and fine roots both participating in nutrient uptake. In contrast, the effective

TABLE 1

Biological parameters

Value	Units	Description	Comment
0.026	cm depth g^{-1} C m^2 y	dchar vs NPP slope	see text
10.1	cm depth	dchar intercept	see text
0.018	m cm^{-3} soil	AM fine root length density	mean temperate forest value derived from Jackson and others (1997)
0.0	m cm^{-3} soil	EM fine root length density	EM trees nutritionally dependent on EM fungi
10^{-6}	mol m^{-1}root day^{-1}	Oxalate exudation by fine roots	Maize, Radersma and Grierson (2004) using data from Jones and Darrah (1995)
10^{-10}	mol m^{-1} hyphae day^{-1}	Oxalate exudation by EM hyphae	*Pinus sylvestris* (van Hees and others, 2006)
2	H^+ per Ox^{2-}	Acidification due to organic anion exudation, range 0–2	$2H^+$, $2K^+$ or one of each will balance the charge of one Ox^{2-}
4.17×10^{-2}	days	residence time of oxalate in soil solution (one hour)	can be less than one hour (van Hees and others, 2005b)
800	g C m^{-2} y^{-1}	NPP for temperate forests today	derived from Saugier and others (2001)
0.018	m root cm^{-3} soil	AM fine root length density today	derived from area-weighted average for temperate forests, Jackson and others (1997)
0.0	m root cm^{-3} soil	EM fine root length density today	EM roots receive nutrients only from EM fungi
5	m AM hyhae cm^{-3} soil	AM hyphal length density today	Klironomos and others (1997) *Populus tremuloides*
125	m EM hyhae cm^{-3} soil	EM hyphal length density today	derived from Wallander and others, 2004 *Quercus robur*
0.29	mm	fine root radius	Jackson and others (1997)
1.4	μm	hyphal radius	van Hees and others (2006)
1.0	dimensionless	AM hyphal length response to CO_2 changes	derived from meta-analysis of Alberton and others (2005)
1.73	dimensionless	EM hyphal length response to CO_2 changes	derived from meta-analysis of Alberton and others (2005)
1.56	dimensionless	AM fine root length response to CO_2 changes	derived from data for *Liquidambar styraciflua* Norby and others (2002)
1.51	dimensionless	EM fine root length response to CO_2 changes	derived from data for *Quercus alba* Norby and others (1986)

EM fine root length density is set to zero (table 1). Over 90 percent of fine root tips of EM trees are isolated from the soil by sheaths of EM mycelium (Pregitzer and others, 2002), and such roots receive all their water and nutrients via the fungi.

We model soil as homogenous above the millimeter scale, lacking highly nutritious patches that might encourage root clumping (Robinson, 1996). The rock fragments in the soil, however, comprise nutrient-rich minerals (table 2) and less nutritious minerals such as quartz in granite. In our model, fine roots acidify the soil solution coating all surfaces in the soil volume calculated by multiplying the characteristic depth by the porosity and saturation for the soil (table 3). This volume is the effective rhizosphere (table 4). AM and EM hyphae are assumed to seek only the nutrient-bearing minerals (Leake and others, 2008) within this volume.

We can easily check that our treatment of rhizosphere volume is reasonable. The rhizosphere can be defined as a hollow cylindrical volume $length_{root} \times \pi(R^2_{rhiz} - R^2_{root})$ surrounding the root, with an extent defined by the depletion of nutrients adjacent to the root. Such a depletion radius is on the order of a few millimeters (Nye, 1981; Li and others, 1991; Marschner and others, 1991; Kim and Silk, 1999; Ryan and others, 2001; Hinsinger and others, 2005). Using the NPP and AM root length density in table 1 and calculating a characteristic depth of 31 cm using equation (3), we solve for an effective rhizosphere radius of 3.9 mm. The characteristic depth therefore provides a simple way to estimate the effective rhizosphere volume while allowing mycorrhizal hyphae to proliferate and form clumps within the same volume. We scale this volume according to the fraction of the surface area comprising the Ca-Mg rich minerals, estimated using the mineralogical data in table 5, to get the volume of the hyphosphere. These effective rhizosphere and hyphosphere volumes are used to calculate H^+ and oxalate concentrations due to fine root and hyphal ion exchange, respectively. The mycorrhizosphere is the union of these volumes.

Soil Water

Substantial quantities of water can be transported by hyphae (Duddridge and others, 1980; Brownlee and others, 1983; Unestam, 1991; Unestam and Sun, 1995; Querejeta and others, 2003) and brought to weathering sites for the purpose of nutrient uptake (Sun and others, 1999). We assume therefore that the soil water content at sites producing high weathering fluxes of Ca and Mg is adequate for weathering by both fine roots and hyphae.

Given the above assumptions, the residence time of the water is an important parameter. We estimated this using the unsaturated hydraulic conductivities measured from the same soils as our porosities and saturations (table 3). The two soils are geographically close together and should experience similar environmental conditions. We allow our soil water volume to vary with the runoff, which is calculated using global parameters available in the original GEOCARBSULF model.

Rate Laws for Mineral Weathering

Given a mineral composition for basalt and granite (table 5), we calculate weathering rates using equations of the form

$$Rate = \sum_{ij} k_{ij} \times a_j^{n_{ij}} \times \exp\left(-\frac{E_{app}}{RT}\right) \tag{7}$$

where the subscripts i and j refer to minerals and weathering agents a (H^+, H_2O, OH^-, CO_3^{2-}, oxalate), respectively, k_{ij} and n_{ij} are experimentally determined parameters, E_{app} is the apparent activation energy, and *Rate* has units of mol(mineral) m^{-2}(mineral) s^{-1}. Using the mineralogical data in table 5, we can convert these weathering rates to release rates of Ca and Mg.

This form of rate law was chosen because such rate laws are readily available for a range of minerals and weathering agents, allowing us to change them easily without the mineral-specific and agent-specific programming necessary for more complex

Table 2

Rate laws

Rock	Mineral	Agent	log(k)	n	Eapp	Reference	Comment
Basalt	Labradorite	H^+	-7.87	0.626	42.1	Palandri and Kharaka (2004)	
Basalt	Labradorite	H_2O	-10.91	0	45.2	Palandri and Kharaka (2004)	
Basalt	Labradorite	OH^-	-15.6	0.572	71.0	Palandri and Kharaka (2004)	albite
Basalt	Labradorite	CO_3^{2-}	-6.959	0.24	45.2	Berg and Banwart (2000)	anorthite; mol Al m^{-2} $hour^{-1}$ × 0.011
Basalt	Labradorite	Oxalate	-12.8	0.75	45.2	Stillings and others (1996)	andesine; mol cm^{-2} s^{-1}×10000
Basalt	Augite	H^+	-6.82	0.700	78.0	Palandri and Kharaka (2004)	
Basalt	Augite	H_2O	-11.97	0.0	78.0	Palandri and Kharaka (2004)	
Basalt	Augite	Oxalate	-9.6	0.29	78.0	Zhang and Bloom (1999)	hornblende
Basalt	Orthopyroxene	H^+	-9.02	0.600	80.0	Palandri and Kharaka (2004)	enstatite
Basalt	Orthopyroxene	H_2O	-12.72	0.0	80.0	Palandri and Kharaka (2004)	enstatite
Basalt	Orthopyroxene	Oxalate	-9.6	0.29	80.0	Zhang and Bloom (1999)	hornblende
Granite	K-feldspar	H^+	-10.06	0.500	51.7	Palandri and Kharaka (2004)	
Granite	K-feldspar	H_2O	-12.41	0.0	38.0	Palandri and Kharaka (2004)	
Granite	K-feldspar	OH^-	-9.68	0.823	94.1	Palandri and Kharaka (2004)	as given by Brantley (2007)
Granite	Andesine	H^+	-8.88	0.541	53.5	Palandri and Kharaka (2004)	
Granite	Andesine	H_2O	-11.47	0.0	57.4	Palandri and Kharaka (2004)	
Granite	Andesine	OH^-	-15.60	0.572	71.0	Palandri and Kharaka (2004)	albite
Granite	Andesine	Oxalate	-12.8	0.75	38.0	Stillings and others (1996)	10000×mol cm^{-2} s^{-1}
Granite	Hornblende	H^+	-7.00	0.600	75.5	Palandri and Kharaka (2004)	
Granite	Hornblende	H_2O	-10.30	0.0	94.4	Palandri and Kharaka (2004)	
Granite	Hornblende	Oxalate	-9.6	0.29	80.0	Zhang and Bloom (1999)	hornblende; Eapp as above
Granite	Biotite	H^+	-9.84	0.525	22.0	Palandri and Kharaka (2004)	
Granite	Biotite	H_2O	-12.55	0.0	22.0	Palandri and Kharaka (2004)	

TABLE 3

Regolith parameters

Value	Units	Description	Reference	Comment
0.6	Tm^2	effective basalt land area today	Dessert and others (2003)	flux-weighted area derived from their Table 2
1.0	m	regolith depth		
0.7		porosity	Wilson (2006)	Nigerian basaltic soil
0.66		saturation	Wilson (2006)	Nigerian basaltic soil
0.009	$y\ m^{-1}$	soil water residence time	Wilson (2006)	Nigerian basaltic soil
0.49		porosity	Wilson (2006)	Nigerian granitic soil
0.7		saturation	Wilson (2006)	Nigerian granitic soil
0.014	$y\ m^{-1}$	soil water residence time	Wilson (2006)	Nigerian granitic soil

formulations. Our rate laws for weathering by H^+, H_2O and OH^- are from the compilation of Palandri and Kharaka (2004). We use the mean annual temperatures produced by GEOCARBSULF, which are slightly lower than the temperature range for which the rate laws were derived (25 °C and over). However, we considered that the use of rate laws derived in a consistent way and including temperature corrections for all of our minerals outweighed the extrapolation to lower temperatures.

TABLE 4

Terms, definitions and abbreviations

AM plant or fungus	Arbuscular mycorrhizal plant or fungus
Arbuscular mycorrhiza	Partnership between a plant and a fungus of Glomeromycota, where the fungus complements rather than replaces the uptake functions of the infected roots. This is the ancestral mycorrhizal type, dating from at least the Devonian.
EM plant or fungus	Ectomycorrhizal plant or fungus
Ectomycorrhiza	Partnership between a tree and a fungus of Basidiomycota or Ascomycota, where the fungus forms sheaths around root tips and takes over all nutrient uptake functions of the infected roots.
Ectomycorrhizosphere	Soil under the influence of ectomycorrhizal fungi and fine roots
Ericoid mycorrhiza	Partnership between an ericaceous plant (such as heather) and a fungus of Ascomycota, replacing the function of root hairs of infected roots.
Hyphosphere	Soil under the influence of mycorrhizal hyphae
Mycelium	Network of hyphae comprising the vegetative parts of a fungus
Mycorrhiza	Mutually beneficial partnership between a plant and a fungus
Mycorrhizosphere	Soil under the influence of fine roots or mycorrhizal hyphae. We use it in a broad sense to refer to any combination of hyphosphere and rhizosphere.
NM plant	Non-mycorrhizal plant
Non-mycorrhizal	Without mycorrhizal fungi of any kind
Rhizosphere	Soil under the influence of fine roots
Tm^2	Square terameters (1 Tm = 10^{12} m)

Table 5

Mineralogical data

Rock	Mineral	Wt%	Ca	Mg	K	Na	Reference
Basalt	Labradorite	0.498	0.508	0.000	0.098	0.394	Nockolds (1954)
Basalt	Augite	0.22	0.42	0.38	0.00	0.00	Nockolds (1954)
Basalt	Orthopyroxene	0.1526	0.05	0.62	0.00	0.00	Nockolds (1954)
Granite	K-feldspar	0.119	0.00	0.00	0.86	0.15	White and others (1996)
Granite	Andesine	0.365	0.33	0.00	0.00	0.64	White and others (1996)
Granite	Hornblende	0.071	1.73	2.25	0.15	0.26	White and others (1996)
Granite	Biotite	0.018	0.13	1.75	0.87	0.33	White and others (1996)

Surface Area

Mineral surface area.—Because weathering rates of fresh mineral surfaces used in experiments are faster than rates measured in the field (for example, White and Brantley, 2003), BET surface areas derived in the laboratory are not appropriate for calculating our weathering fluxes. We therefore decided to generate surface area calibration curves for basalt and granite for the Phanerozoic.

Under the assumption that the GEOCARBSULF model (Berner, 2006a, 2006b, 2008) is valid, we ran our model using the original GEOCARBSULF silicate flux functions, but also generating weathering rates using our rate laws. Comparison of the silicate weathering flux F_{wsi}, which is the difference between carbonate burial and carbonate weathering in GEOCARBSULF, and our weathering rates allowed us to generate calibration curves for basalt and granite for the Phanerozoic for a chosen baseline case. Our rates have units of mol m^{-2}(mineral) s^{-1} so the correction factor at each time-step depends on the length of the growing season. We then used these calibration curves to generate fluxes for non-standard cases in our sensitivity analyses.

For basalt, this calibration curve (fig. 6A) varies between 18000 to 26000 m^2(mineral) m^{-2}(land) for the last 200 Ma. This compares favorably with the scaling value of 20000 derived by Navarre-Sitchler and Brantley (2007) for conversion between laboratory and watershed basalt weathering rates. Our curve for granite (fig. 6B) is lower, which is not surprising given published BET surface areas of 8.69 $m^2\ g^{-1}$ basalt and 0.14 $m^2\ g^{-1}$ granite (Neaman and others, 2006). As shown, the use of a shorter growing season for granites may have been appropriate, given rocks with similar composition such as gneisses may be found in mountainous regions at higher altitudes and be subject to seasonal influences to a greater extent than basalts. Our baseline growing season is one full year (aseasonal conditions). Therefore, our calibration curves represent the combined influences of mineral surface area and seasonality. They also reflect the signature of the erosion function (Berner, 2004) used in GEOCARBSULF (figs. 6A and 6B). The resulting CO_2 curve matches the GEOCARBSULF model everywhere within the last 200 Ma.

Land surface area.—Bluth and Kump (1991) estimated basalt and "shield" (granitoid) land exposure areas for the Phanerozoic, but the shield areas in particular are known to be underestimated (Gibbs and Kump, 1994; Gibbs and others, 1999). Many exposures are covered by old or thick soils and are not undergoing far-from-equilibrium weathering (Stallard, 1995; Hodson and others, 1998; Hodson and Langan, 1999; White and Brantley, 2003; White and others, 2005; Goddéris and others, 2008). Other areas are either too cold or too dry. Large areas of flood basalts, including the Siberian Traps, are not producing substantial weathering fluxes today (Dessert and others, 2003), and the warm, wet Amazon watershed produces surprisingly low Ca and Mg fluxes for its area (Gaillardet and others, 1999). Hartmann and others (2009) have highlighted the role of very active weathering sites, noting that only

9 percent of the world's exorheic area accounts for half the CO_2 consumption by chemical weathering. In light of these problems, we do not use any available estimate of global rock area. Instead, we calculated a flux-weighted effective modern land area $(\sum Area_i \times Flux_i)/(\sum Flux_i)$ of 0.6 Tm^2 (table 3) for basaltic provinces derived from table 2 of Dessert and others (2003). We then estimate a granite (shield) area using existing parameters of the GEOCARBSULF model (Berner, 2006b, 2008): an estimate of the relative weatherability of basalt and granite ("VNV"=2), and the fraction of Ca and Mg derived from volcanic as opposed to other silicate weathering ("Xvolc"). With these effective areas, our calibration curves, and a function describing the variation of the total weatherable (non-ice, non-desert) land area over the Phanerozoic, we calculate global fluxes of Ca and Mg from basalt and granite.

Distribution of Mycorrhizal Functional Types

We chose a baseline case likely to reflect the prevalence of EM trees and shrubs at higher altitudes in watersheds, such as the Irrawaddy, and in Southeast Asian rainforests, where EM dipterocarps are often the dominant trees today.

Although only about 3 percent of modern vascular plant species are EM, these are the dominant trees of boreal and temperate forests (Read, 1991), which comprise almost 50 percent of global forested land area (Jackson and others, 1997). The other 50 percent includes regions such as the AM-dominated Amazon lowlands, which contribute little to global Ca and Mg fluxes per unit area (Gaillardet and others, 1999), but some tropical forests are dominated by EM trees. Mountainous watersheds with high Ca and Mg fluxes may have a much higher proportion of EM vegetation. For example, the Irrawaddy watershed in Southeast Asia is the largest producer of Ca and Mg from silicate weathering (Gaillardet and others, 1999) and the mountain forests are dominated by the Pinaceae and Fagaceae (Blasco and others, 1996), with rhododendrons at higher altitudes. Rhododendrons are members of the Ericaceae and they have ericoid mycorrhizal fungi, which, like ectomycorrhizal fungi, exude LMWOAs and acidify their hyphospheres (Martino and others, 2003). The ericoid mycorrhiza is probably derived from the ectomycorrhiza (Brundrett, 2002; Wang and Qiu, 2006). It involves fungal species of Ascymycetes and Basidiomycetes, some of which can form both ericoid and ectomycorrhizas (Smith and Read, 2008), so these fungi may resemble EM fungi more closely than AM fungi in a weathering context. Additionally, parts of the middle and lower reaches of the Irrawaddy watershed are dominated by the EM family Dipterocarpaceae.

Berner (1991, 1994) assumed that angiosperms radiated between 130 to 80 Ma. This radiation began at low latitudes (Crane and Lidgard, 1989) but angiosperms were minor components of the total flora at mid to high latitudes before about 100 Ma (Lidgard and Crane, 1990). Angiosperm wood is rare until the end of the Cretaceous (Wing and Boucher, 1998), suggesting that many early angiosperms were herbaceous. The mycorrhizal status of these early angiosperms was likely to be AM, although Moyersoen (2006) suggests that the ancestors of the dipterocarps were EM prior to the separation of Africa from South America at about 135 Ma, and Ducousso and others (2004) note that the last common ancestor of the EM families Sarcolaenaceae and Dipterocarpaceae must have been EM prior to the separation of India and Madagascar at about 88 Ma. Cretaceous ancestors of these families have not been confirmed in the fossil record. Sarcolaenaceae, presently endemic to Madagascar, is known only from pollen in Miocene deposits in South Africa (Nilsson and others, 1996), and the Cambay ambers of Gujarat (52-50 Ma) comprise the earliest physical evidence of Dipterocarpaceae to our knowledge (Rust and others, 2010). We note that these trees are not known to be pollinated by wind (Ashton, 2003; Bayer, 2003) and their pollen is therefore unlikely to be common in the palynological record; we also expect the

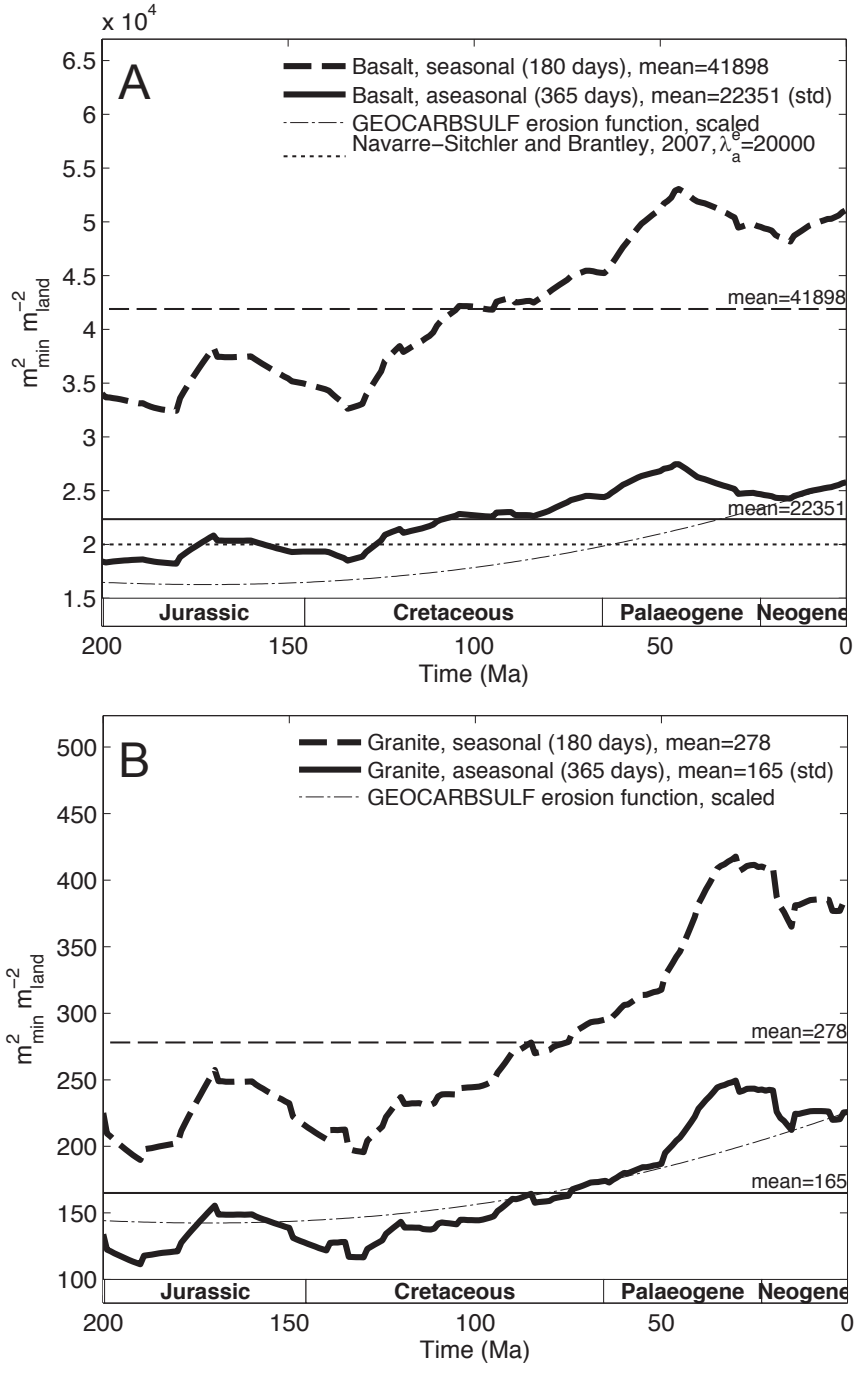

Fig. 6. Effective mineral surface area on (A) basalt and (B) granite. The "roughness" for basalt watersheds of 20000 published by Navarre-Sitchler and Brantley (2007) is shown for comparison. Our curves include errors in the global effective growing season length for weathering hotspots. Aseasonal conditions are represented by the lower curves in each panel; the upper curves indicate seasonality.

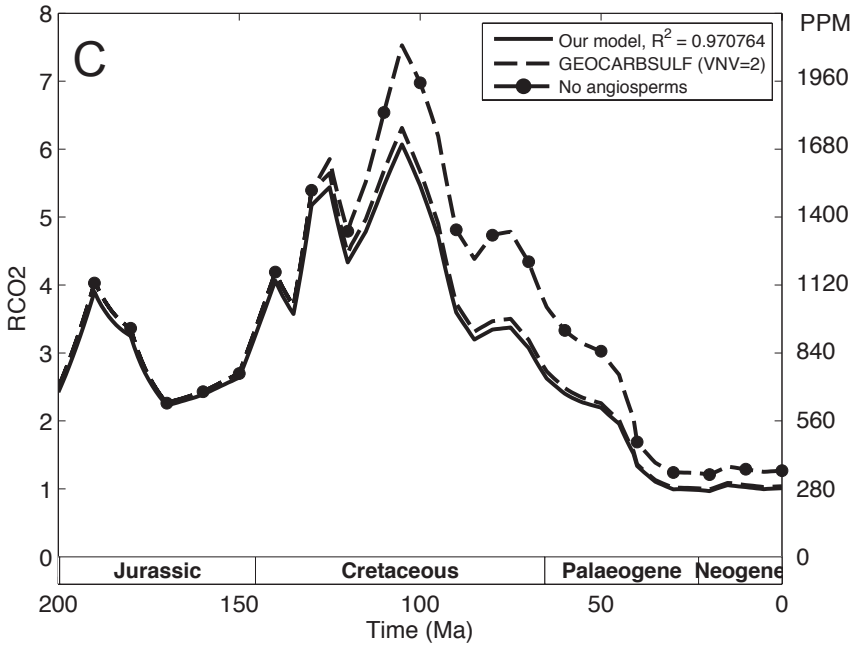

Fig. 6. (continued). (C) Using these calibration curves, we can force our baseline case to match GEOCARBSULF (Berner, 2006b) throughout the Phanerozoic with the exception of the Devonian, where GEOCARBSULF (Berner, 2006b) linearly interpolates between an abiotic feedback function given by $RCO2^{0.5}$ in the lower Paleozoic and a Michaelis-Menten function from the Carboniferous onward. We also generated a "no angiosperm" curve with GEOCARBSULF (Berner, 2006b) by holding the dimensionless plant weathering efficiency function at the putative pre-Cretaceous gymnosperm value (f_E=0.875) for the last 200 Ma. The standard value for modern vegetation is f_E=1.

preservation potential of vegetative structures to be poor in the warm, moist conditions which are especially conducive to weathering.

Other modern EM angiosperm families, such as Betulaceae and Fagaceae, do not appear in the fossil record until the Turonian, Santonian or Campanian (Wing and Boucher, 1998) in the late Cretaceous. It is therefore possible that EM angiosperms may not have made a significant contribution to CO_2 drawdown until the late Cretaceous or early Cenozoic. In the early Cretaceous, EM Gnetales experienced a radiation at low latitudes (Crane and Lidgard, 1989), whereas fossils of the EM family Pinaceae were widespread in the northern hemisphere, especially Siberia (Vakhrameev and Hughes, 1991). This implies that EM weathering would have been driven first by gymnosperms, and then by mixed vegetation. Our baseline case therefore assumes that EM trees begin to displace the ubiquitous AM vegetation at weathering hotspots from the Cretaceous onwards.

There were also numerical reasons for choosing the more aggressively weathering EM vegetation as the baseline case: if too much CO_2 is drawn down, then the RCO2 curve will reach a lower limit. This is defined as RCO2=0.7 (~200 ppm), as root biomass and NPP decline sharply below this CO_2 concentration (Pagani and others, 2009). Our choice allowed investigation of the relative change in the CO_2 curve for scenarios ranging from 100 percent AM to 100 percent EM, and with a range of other parameters such as hyphal length density, without having our results compromised by this issue.

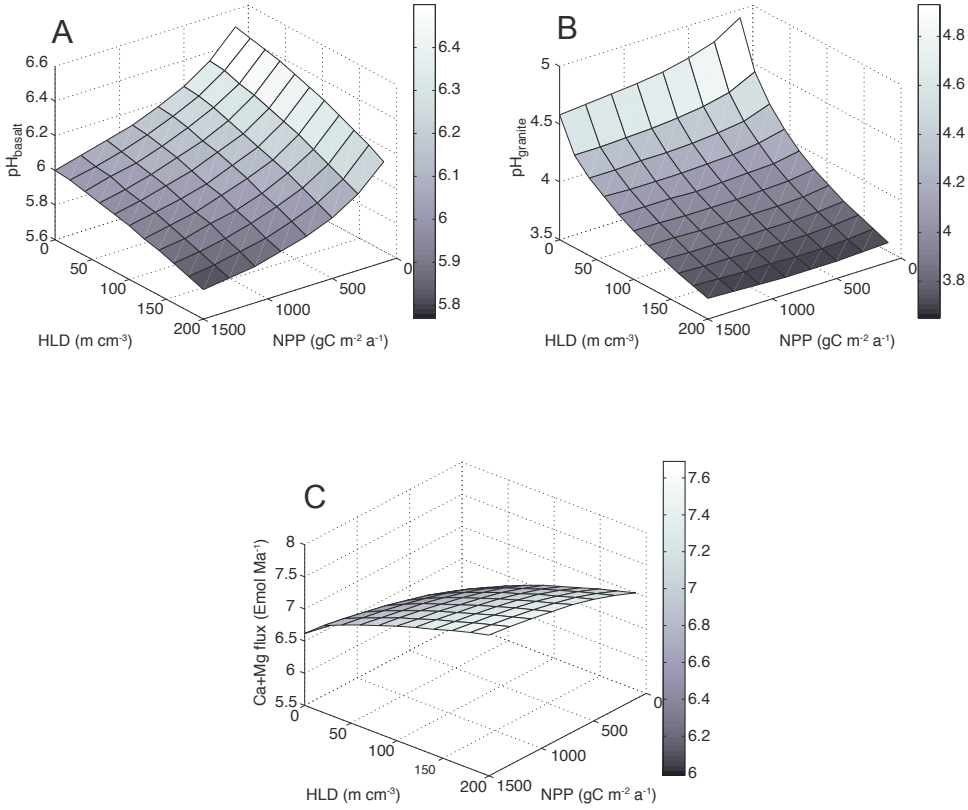

Fig. 7. Effect of net primary productivity and ectomycorrhizal hyphal length density on pH in the mycorrhizosphere (A) on basalt and (B) on granite. We used our baseline calibration curves in both cases, and assumed that H^+ was the counter-ion for low molecular weight organic anions (modeled as oxalate). (C) The resulting calcium and magnesium fluxes from EM vegetation.

RESULTS

We first conducted a series of sensitivity analyses, generating surfaces (figs. 7 and 8) to determine the simulated effects of model parameters on mycorrhizosphere pH and flux of calcium and magnesium. These simulations were done for the preindustrial present at 0 Ma with parameters for the baseline case shown in tables 1, 2, 3 and 5. We then explore the effects of parameters related to EM fungi on the long-term carbon cycle (fig. 9). These parameters are EM oxalate exudation rate, EM hyphal length, and the percentage of EM vegetation at weathering sites.

Baseline case.—As described above, we assume that sites producing high fluxes of Ca and Mg (weathering hotspots) have 100 percent EM vegetation growing on soils derived from basalt or granite today, and that EM trees began to displace AM vegetation at such hotspots in the Cretaceous. Also, we assume that ammonium was the dominant form of nitrogen taken up by our plants and fungi. Our oxalate exudation rates for AM roots and EM hyphae are fixed values chosen from the literature (Radersma and Grierson, 2004; van Hees and others, 2006) and oxalate is assumed to have an acidifying effect (Arvieu and others, 2003; Casarin and others, 2003). We also set modern values for NPP, fine root length density, and the hyphal length density for both mycorrhizal functional types (table 1); these parameters will vary with atmo-

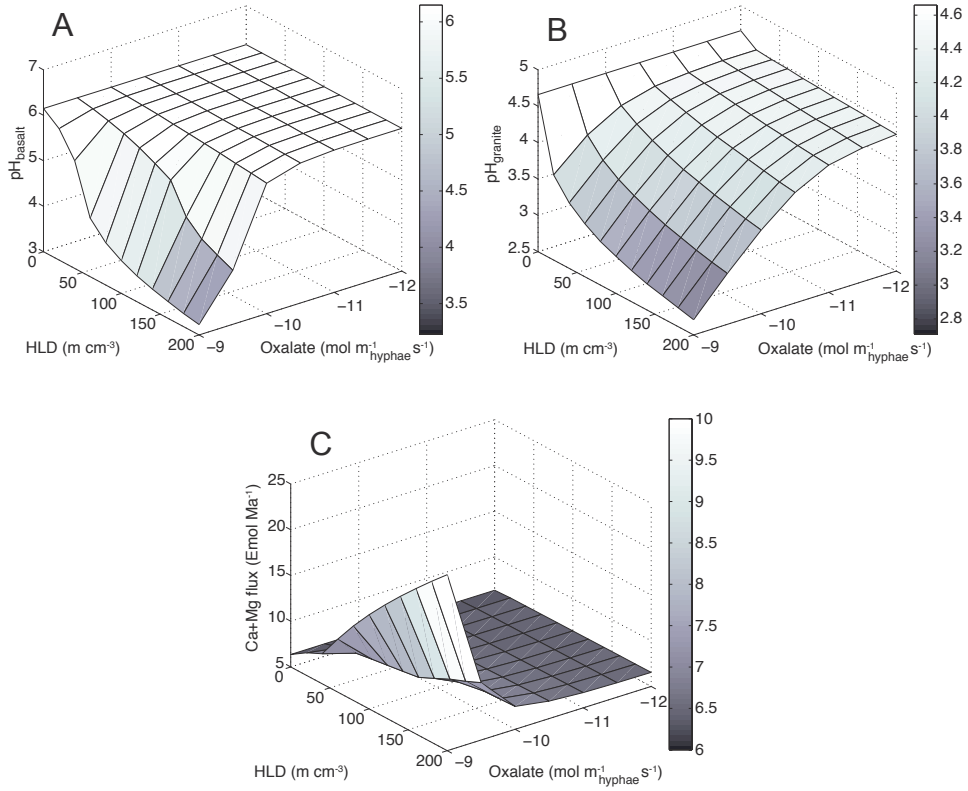

Fig. 8. Effect of changing ectomycorrhizal hyphal length density and oxalate exudation rate for a fixed net primary productivity (NPP) of 800 gC m^{-2} y^{-1} on mycorrhizosphere pH (A) on basalt and (B) on granite. (C) Global Ca+Mg fluxes are largely insensitive to oxalate at our standard exudation rate of 10^{-10} mol m^{-1} (hyphae) day^{-1}, but for higher exudation rates fluxes rise sharply.

spheric CO_2 levels as described above. Parameters inherited from GEOCARBSULF retain their original values in our model.

AM case.—Pre-Cretaceous vegetation comprises AM gymnosperms. Unlike EM roots, AM roots participate in nutrient uptake and exude organic acids, whereas AM hyphae do not exude organic acids. AM hyphal lengths are also significantly shorter than EM hyphal lengths (Leake and others, 2004). In the AM case, no EM vegetation displaces the AM vegetation; it is created by setting the percentage of EM vegetation to zero for all time and then running our model with the same parameters and calibration curves as for the baseline case.

No angiosperm case.—We also generated a CO_2 curve for the scenario where vegetation does not change since the Jurassic using the GEOCARBSULF model (Berner, 2006a, 2006b, 2008). In the GEOCARB family of models (Berner and Kothavala, 2001; Berner, 2006a), increased drawdown of atmospheric CO_2 beginning in the Cretaceous is expressed with an empirical plant weathering efficiency function f_E. Modern vegetation is assigned $f_E = 1.0$, whereas pre-Cretaceous vegetation is assigned $f_E = 0.875$. We fixed $f_E = 0.875$ until the present day in GEOCARBSULF (fig. 6C) to generate our putative "no angiosperm" curve. If the spread of EM vegetation is responsible for the CO_2 drawdown, then our AM curve should match this "no angiosperm" curve.

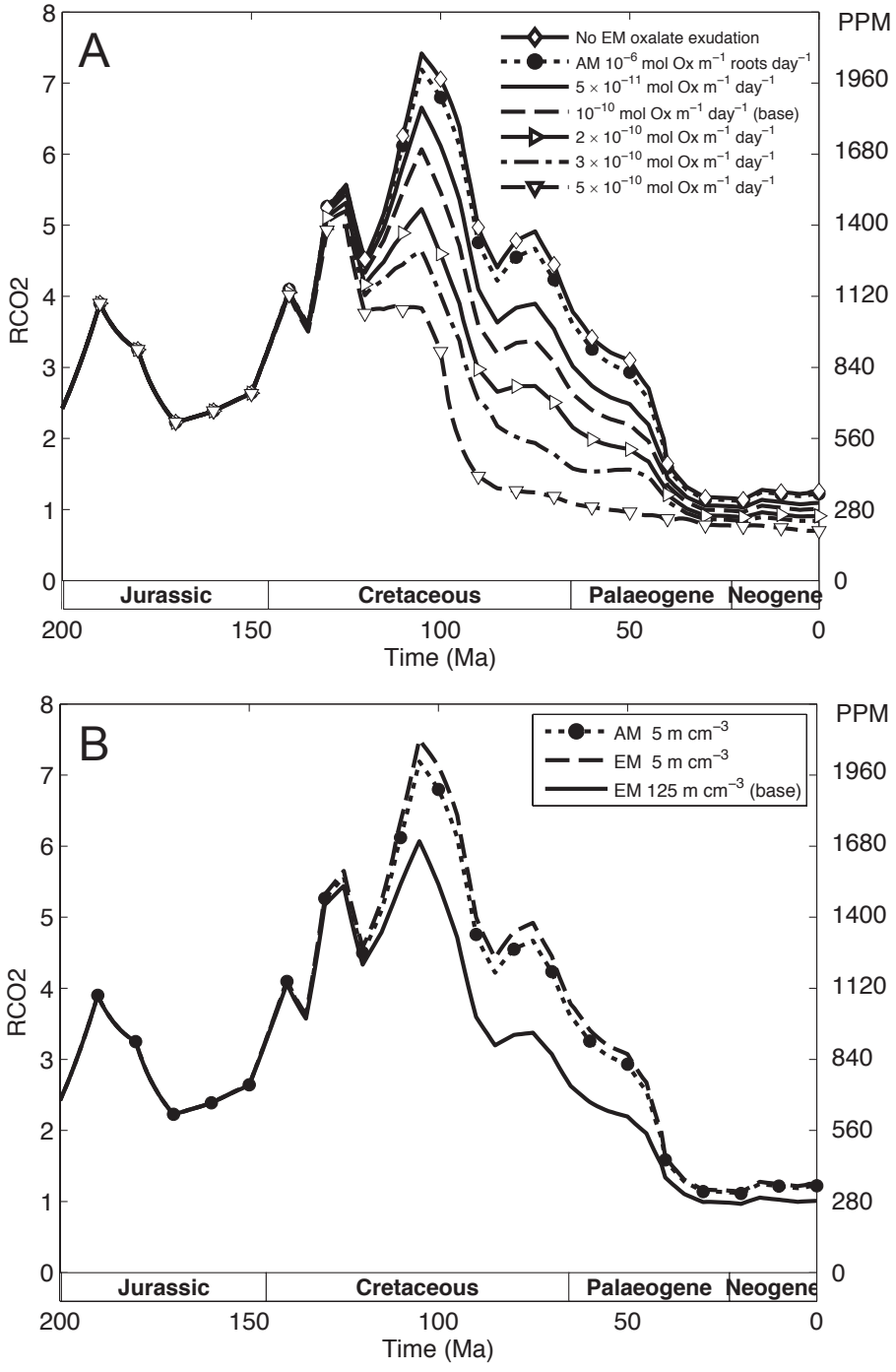

Fig. 9. Sensitivity of atmospheric CO_2 to (A) organic acid exudation rate from ectomycorrhizal (EM) hyphae, (B) EM hyphal length density, and (C) percentage of EM vegetation at weathering hotspots. Figure (A) shows the behavior we expect from examination of fig. 8C, where high exudation rates lead to high Ca+Mg fluxes and dramatic drawdown of CO_2.

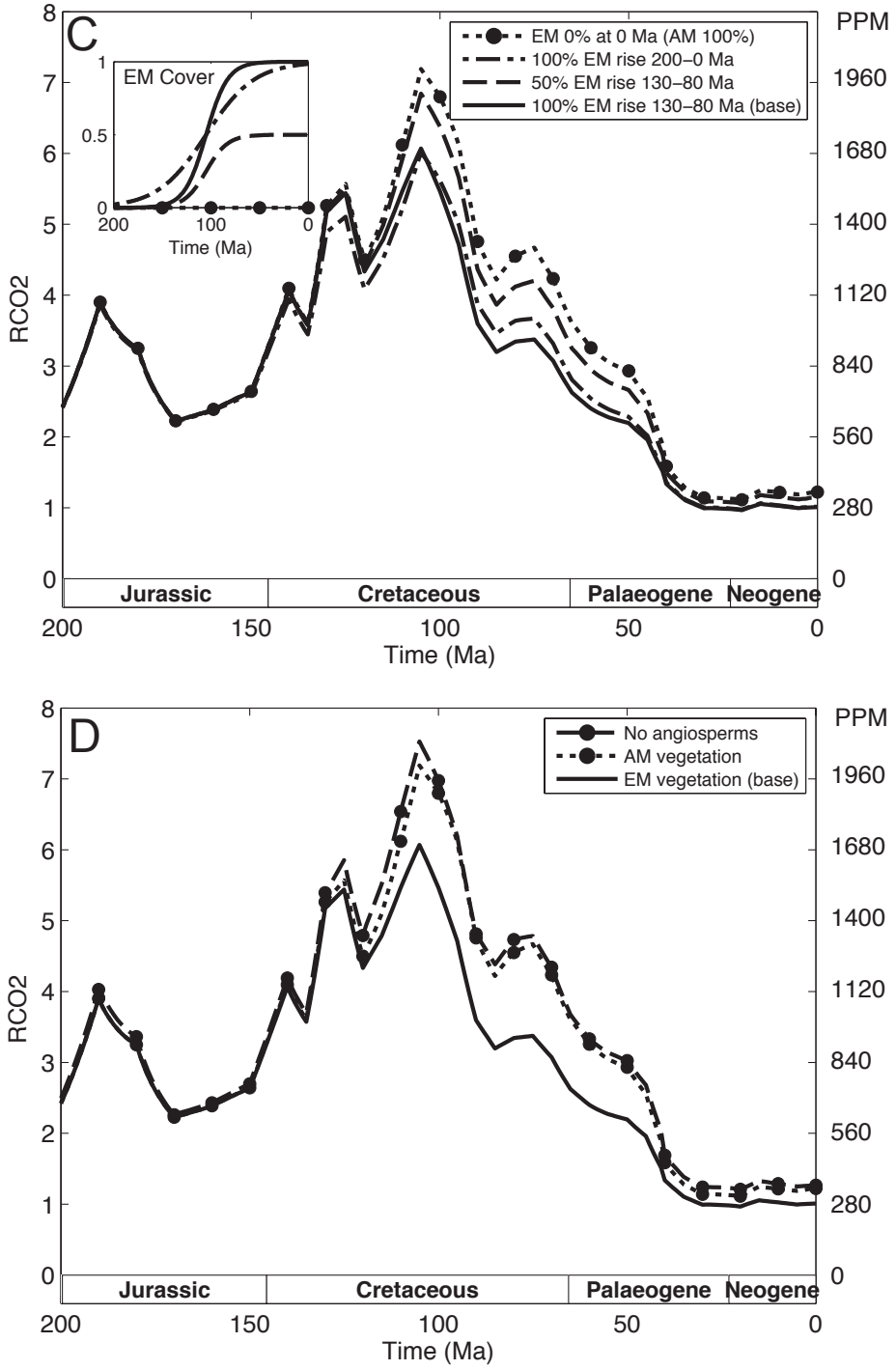

Fig. 9. (continued). If EM fungi exude no oxalic acid, or if EM hyphal lengths are as low as arbuscular-mycorrhizal (AM) hyphal lengths (C), then the EM and AM curves are comparable. Similar effects occur (C) if EM is not the dominant mycorrhizal functional type. The inset shows the sigmoidal EM cover function used in our baseline case, as well as several alternative functions. (D) The "no angiosperm" curve (also shown in fig. 6C) closely matches our AM case (R^2=0.9922 for t≤200 Ma), suggesting that the effect of EM fungi on weathering could account for the entire CO_2 drawdown attributed to the spread of angiosperms at the expense of gymnosperms in the GEOCARB family of models.

Effects of EM Fungi on Soil Chemistry—Sensitivity Analyses

NPP, hyphal length density and pH.—Our conceptual model indicates that the pH of the mycorrhizosphere should decrease as biological net primary productivity (NPP) increases through enhancement of the biological proton cycle (fig. 2), resulting in higher fluxes of calcium and magnesium. We also expect that pH will drop with increasing EM hyphal length density (HLD), while the flux of calcium and magnesium should rise. Sensitivity analysis of the model using the baseline case at 0 Ma produces the surfaces in figures 7A and 7B that show the magnitude of these effects of NPP and HLD on basalt and granitoid rocks, respectively. Weathering fluxes of Ca+Mg (fig. 7C) rise with increasing NPP and EM HLD.

Oxalate exudation rate and pH.—We produced pH surfaces for basalt (fig. 8A) and granite (fig. 8B) assuming that oxalate anions were accompanied by H^+ as observed by Arvieu and others (2003) and Casarin and others (2003). Note that if the oxalate exudation rate is larger than our baseline rate of 10^{-10} mol m^{-1}(hyphae) s^{-1}, then the pH on basalt drops very steeply. Fluxes of calcium and magnesium mirror the effect seen in figure 8A, rising sharply in concert with increasing oxalate exudation rate.

Effects of EM Weathering on Atmospheric CO_2 Over the Last 200 Ma

Oxalate exudation rate.—Our model is very sensitive to high LMWOA exudation rates (fig. 9A), and if exudation rates were an order of magnitude higher than our baseline case, the RCO2 curve would be flattened to such an extent that there would be insufficient atmospheric CO_2 to support widespread forests for much of the Cenozoic. This extreme case is not necessarily reasonable, as the LMWOA exudation rate is a constant in our model which does not respond to environmental parameters. Also, our search algorithm will stop at a borderline RCO2=0.7 as explained above. Note that the shape of the curve is largely unchanged, as this is controlled by the seafloor spreading data (Berner and Kothavala, 2001).

EM hyphal length density and EM cover.—EM hyphal length density (fig. 9B) and EM percentage cover (fig. 9C) exert a less dramatic influence, potentially changing the height of the curve by over one RCO2 unit in the Cretaceous if hyphal lengths remain small or EM vegetation does not spread. Intermediate effects occur when the spread of EM vegetation (see inset, fig. 9C) to rapidly-weathering regolith is less than 100 percent at 0 Ma. For our baseline case, we use a logistic curve covering the same timespan (130-80 Ma) for the increase in EM cover as that associated with the spread of angiosperms (Lidgard and Crane, 1988). This is the timespan for which Berner and Kothavala (2001) showed an increase in weathering efficiency leading to drawdown of atmospheric CO_2. Our curve was created with the *sigmf* function in the Matlab® Fuzzy Logic Toolbox, with the inflection point at 105 Ma and the parameter $a = -0.09$, and it has the same slope as the linear function employed in the GEOCARB models (Berner and Kothavala, 2001). We also show the effect of using a wider timespan accounting for Jurassic and earliest Cretaceous fossils associated with Pinaceae (Vakhrameev and Hughes, 1991) and a possible delay in the spread of EM angiosperm trees until the latest Cretaceous or early Cenozoic as described above. Lower EM cover (inset, fig. 9C) always results in less weathering and higher atmospheric CO_2 (fig. 9C). The AM curve (0% EM) generated for this baseline cover function closely resembles the "no angiosperm" curve created with GEOCARBSULF (fig. 9D), implying that the rapid spread of EM vegetation during the Cretaceous could wholly explain the postulated "angiosperm effect" presently incorporated in GEOCARBSULF.

Weathering agents.—Oxalate concentrations rise considerably in the mycorrhizosphere on basalt (fig. 10A), while pH drops in the mycorrhizosphere on granite (fig. 10B) as EM vegetation spreads to weathering hotspots during the Cretaceous, but these curves do not tell us where the Ca and Mg fluxes are coming from, or how. Which

weathering agents, and which minerals, are responsible for most of the drawdown of atmospheric CO_2? On basalt, the largest flux of Ca comes from hydrolysis and carbonate chelation (Berg and Banwart, 2000) of plagioclase, with protons and oxalate providing only minor contributions. Augite is the next largest contributor of Ca and Mg on basalt, producing fluxes an order of magnitude lower than plagioclase. The most important mineral in granite is hornblende, which has the highest rate constant (table 2) and the highest Ca and Mg content (table 5), and this is where we see a noticeable difference in relative Ca and Mg fluxes from the mycorrhizosphere between the standard EM case and our AM and non-mycorrhizal cases. In our simulations, CO_2 is adjusted until the Ca+Mg flux from silicate weathering equals the difference between carbonate burial and carbonate weathering, so that the Ca+Mg flux must be the same for different model runs, but the proportion coming from the mycorrhizosphere and bulk soil on basalt and granite may vary (fig. 11). Comparison of the fluxes from proton-promoted weathering of hornblende (figs. 10C and 10D) and total flux from the mycorrhizosphere on granite (fig. 11) between the baseline and AM cases indicate that weathering of hornblende (table 5) by EM fungi largely controls the drawdown of CO_2 attributed to the spread of angiosperms in the Cretaceous.

DISCUSSION

The spread of angiosperms at the expense of gymnosperms has been postulated for over two decades (Knoll and James, 1987; Volk, 1989; Berner and Kothavala, 2001) to have affected the long-term carbon cycle by contributing to the long-term decline in CO_2 over the past 200 Ma, but the evidence for this is limited (Berner, 2004). However, evaluation of this hypothesis has come from empirical functions implemented in geochemical carbon cycle models, rather than an explicit quantitative consideration of the processes involved. We have investigated the alternative hypothesis (Taylor and others, 2009) that the rise of ectomycorrhizal fungi forming symbiotic partnerships with trees that originated and spread over this same interval are involved in enhancing biotic weathering processes.

Our modeling allows us to test our EM weathering hypothesis, linking our model to core feedbacks and assumptions of GEOCARBSULF. They allow us to investigate relative effects, given that the GEOCARBSULF curve is a product of changing actual conditions, which we treat as our baseline case. According to our simulations, the spread of EM vegetation in the mid-Mesozoic could have been responsible for all or part of this drawdown, depending on weathering rates in the mycorrhizosphere (see below). However, we do not exclude the possibility that the spread of angiosperms operated in concert with the spread of the EM symbiosis on the long-term carbon cycle. The higher evapotranspiration rates of modern angiosperms compared to basal angiosperms and other vegetation (Boyce and others, 2009) may have affected weathering regimes. Runoff may be defined as the difference between precipitation and evapotranspiration (for example, Banwart and others, 2009), so we expect higher evapotranspiration rates to lead to drier soils and possibly to lower weathering rates, unless the resulting higher precipitation falls in the same location. Increased precipitation and erosion with shorter soil water residence times could increase weathering rates. The runoff function in GEOCARBSULF is partly derived from the global climate model (GCM) simulations of Otto-Bliesner (1995). However, as her study excluded the effect of vegetation it is presently difficult to test this "angiosperm evapotranspiration" hypothesis.

In our simulations, we assume that monolithological, young soils with low clay content are the sole source of Ca and Mg to the oceans from silicate weathering. Because we neglect any contributions from sedimentary rocks or regions that are dry, cold, or blanketed with old, thick soils, our chemistry model is less suitable for predicting fluxes from individual watersheds (for example, Banwart and others, 2009;

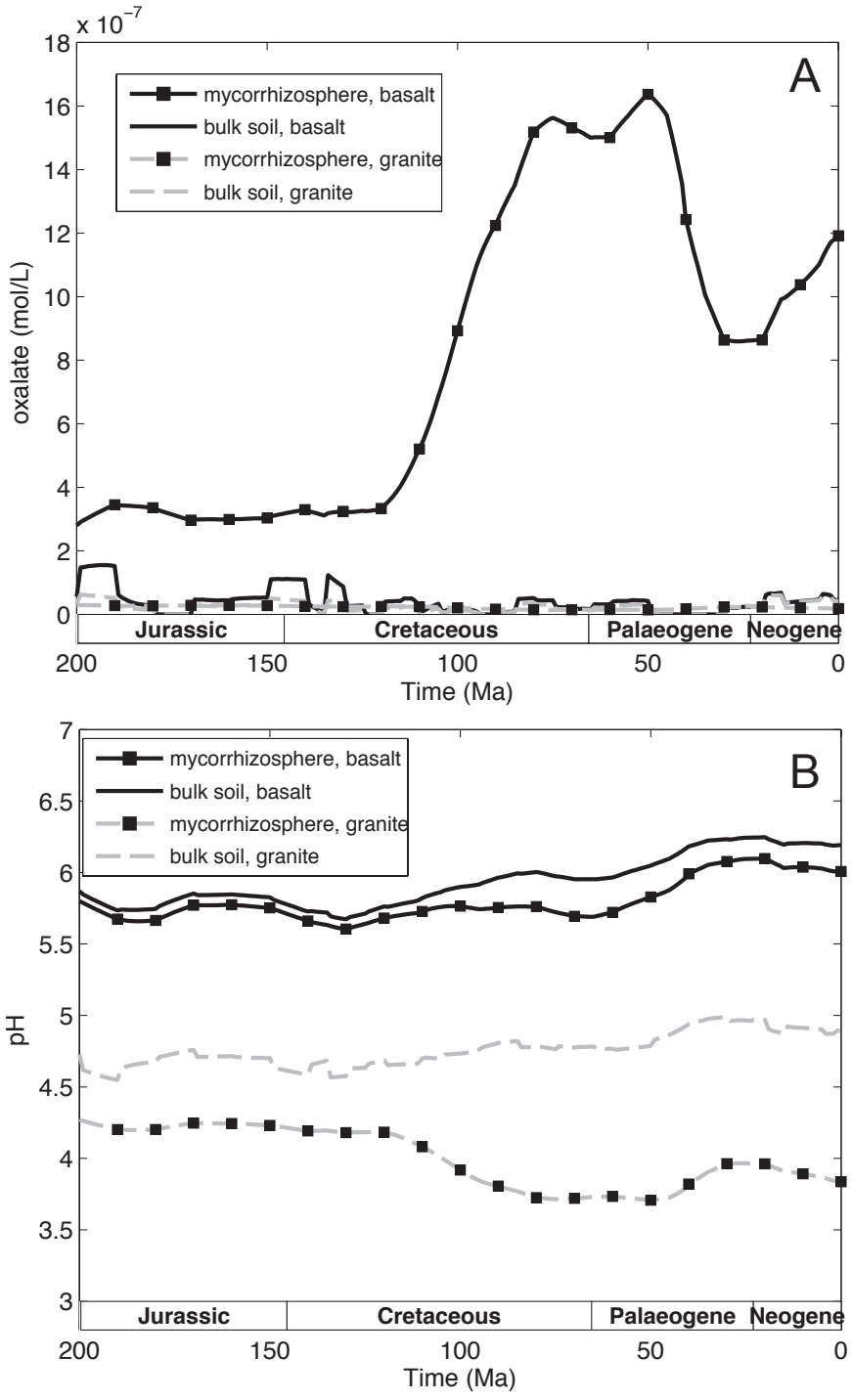

Fig. 10. (A) Oxalate concentrations in the mycorrhizosphere increase with time on basalt but not on granite, whereas (B) pH falls with time in the mycorrhizosphere on granite. In practice, weathering for the base case is largely driven by agents other than oxalate because exudation rates are low. On basalt, most of the calcium and magnesium flux is from plagioclase (modeled as labradorite) undergoing hydrolysis and attack by carbonate ions (Berg and Banwart, 2000).

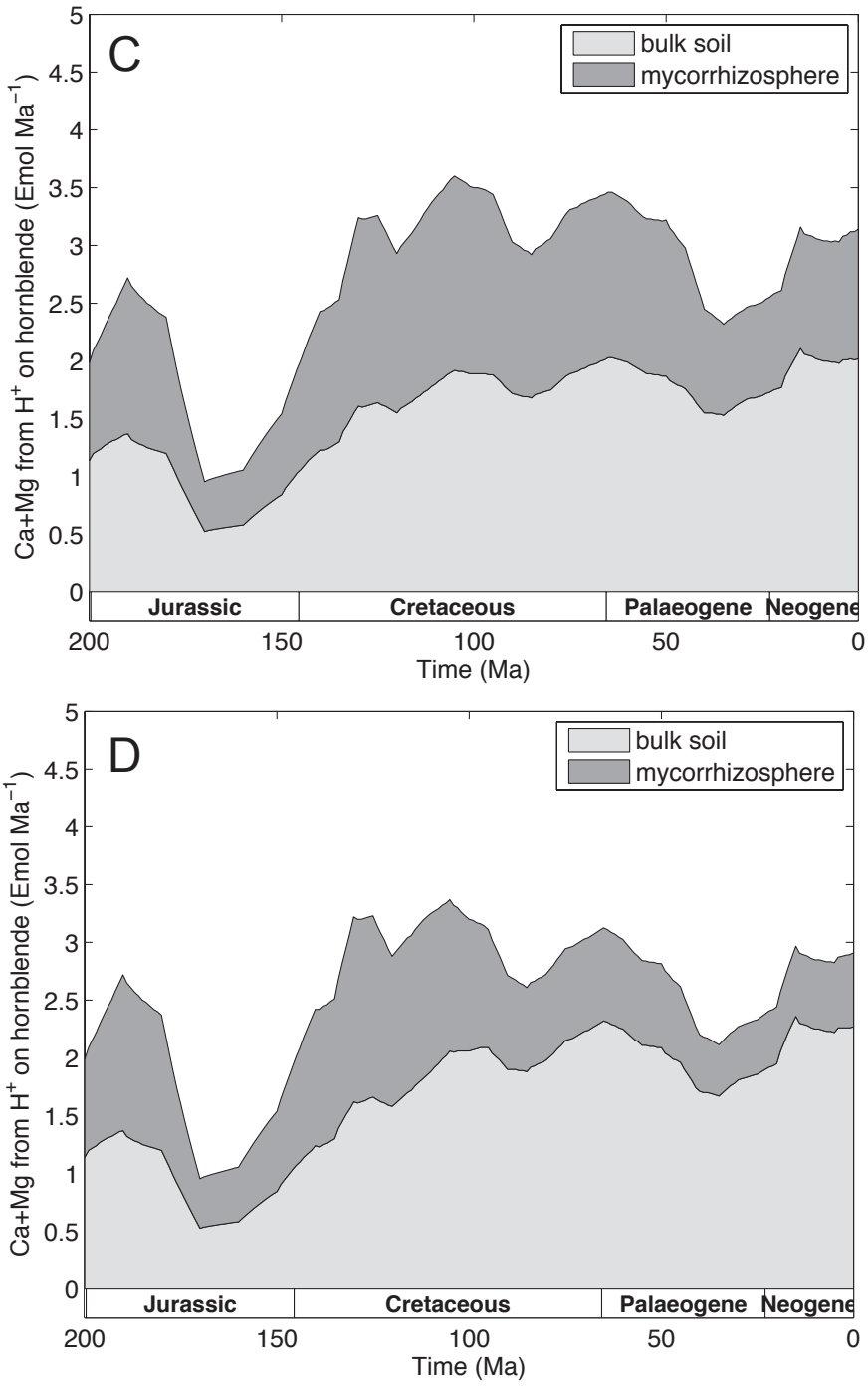

Fig. 10. (continued). Proton-promoted weathering (C, D) and hydrolysis of hornblende are the main contributors on granite. The mycorrhizosphere of the baseline EM case (C) produces greater fluxes from hornblende than that of the AM case (D).

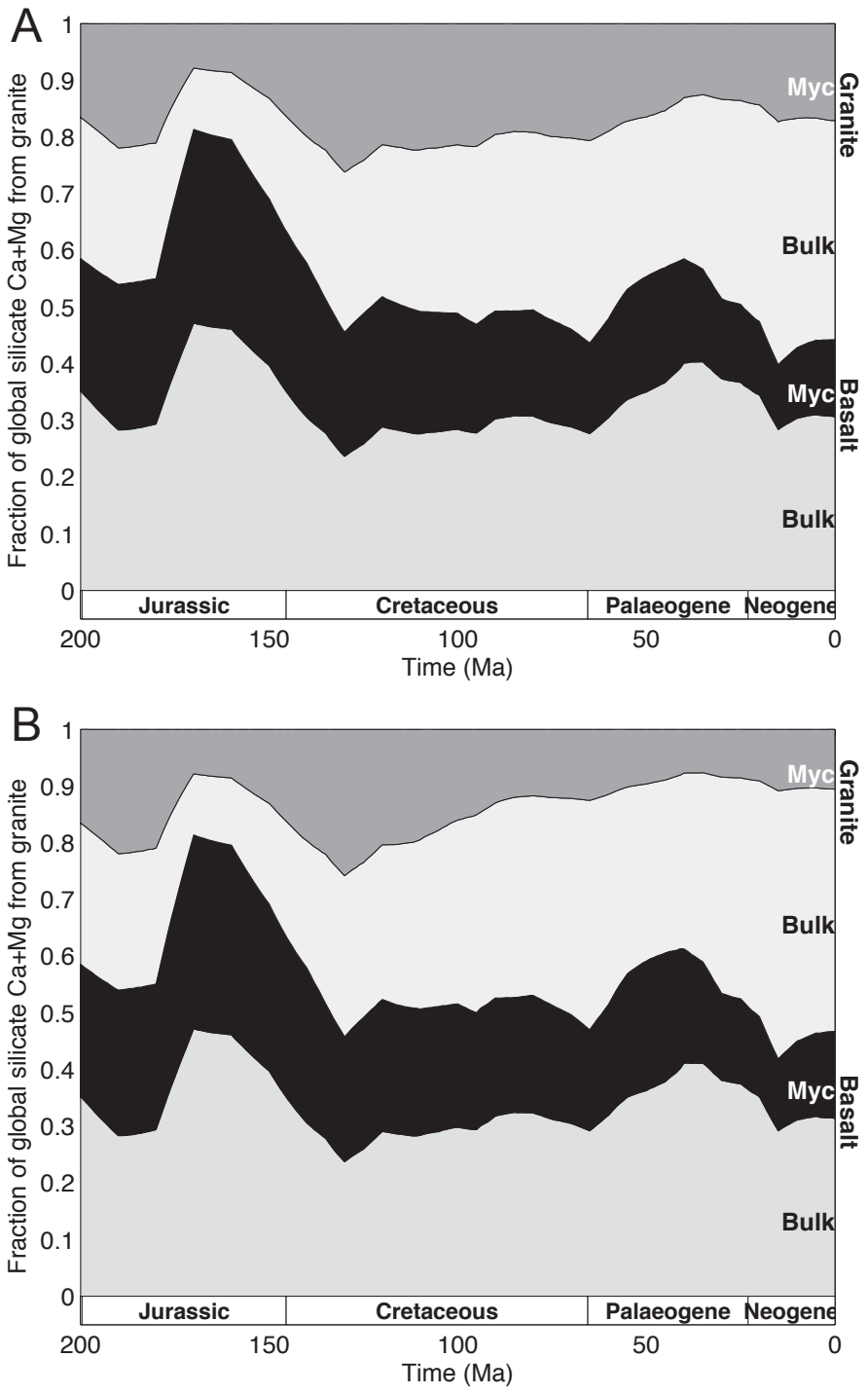

Fig. 11. The fraction of global Ca and Mg coming from the mycorrhizosphere (Myc) on granite for the baseline EM case (A) is larger than that of the AM case (B).

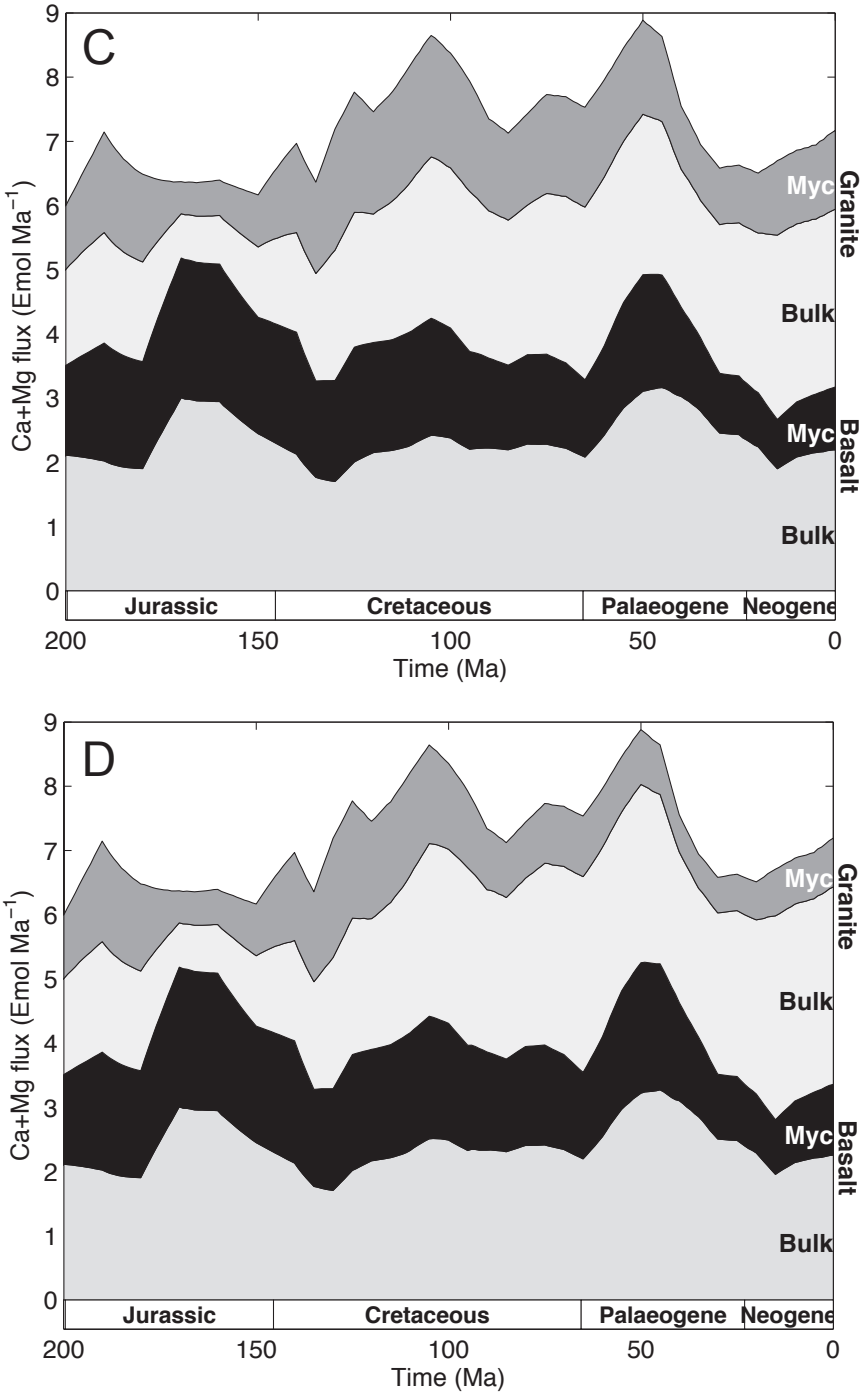

Fig. 11. (continued). The total flux from all soil zones on both rock types for both the baseline EM (C) and AM (D) cases does not vary as it is forced to match the flux as calculated from carbonate weathering and burial by adjusting the level of atmospheric CO_2.

Roelandt and others, 2010). Nevertheless, it provides a first-order way to account for the enhancement of weathering due to the distribution, proliferation and biosensing behavior of fungi at the scale of individual mineral grains compared to roots, despite using rate laws developed for bulk solution weathering.

An important advantage of our approach is its simplicity, and its ability to generate fluxes, weathering rates and geochemical parameters over geological time spans quickly and easily, with a minimum of site-specific parameters. In addition to its current application, it would be useful for sensitivity analyses at a regional and even relatively local scale, so is not limited to one-dimensional, global scenarios.

CONCLUSIONS

Our model analyses indicate that the spread of ectomycorrhizal fungi could have played a key role in the drawdown of atmospheric CO_2 in the Cretaceous and Palaeogene by enhancing biotic weathering processes in the sub-surface environment. This conclusion is strengthened if ectomycorrhizal trees are the dominant vegetation at sites underlain by regolith of granitic composition with rapidly-weathering hornblende, or if they are present as a part of the vegetation and have high rates of low molecular weight organic acid exudation. The mechanisms by which EM fungi could produce higher weathering fluxes of Ca and Mg include the exudation of organic acids and nutrient uptake, and these are adequately captured by our model. Such mechanisms are incorporated in our simple model without invoking any untested or hypothetical processes, such as unknown rate laws operating at a non-aqueous fungal-mineral interface. Our results indicate that mycorrhizal functional type is a viable forcing mechanism for the long-term carbon cycle that should not be ignored. We suggest ectomycorrhizal fungi have the potential to enhance biotic weathering processes to an extent that was previously underappreciated, providing a more plausible mechanism than the spread of angiosperms for biologically-mediated CO_2 drawdown over the last 200 Ma.

ACKNOWLEDGMENTS

We acknowledge funding of this research through NERC award NE/E015190/1 and NERC/World Universities Network consortium award NE/C521001/1. Lyla Taylor was supported by a Hossein-Farmy studentship at the University of Sheffield linked to these grants. David Beerling gratefully acknowledges support from a Royal Society-Wolfson Research Merit Award. We are grateful to Robert Berner for providing the code for his updated GEOCARBSULF and GEOCARB III models, and to Ken Caldeira for sharing his own translation of GEOCARBSULF with us. We thank Adele Duran for her work on the experimental microcosm system shown in figure 1. Helpful comments and suggestions from Dana Royer and two anonymous reviewers led to significant improvements in our manuscript.

REFERENCES

Alberton, O., Kuyper, T. W., and Gorissen, A., 2005, Taking mycocentrism seriously: mycorrhizal fungal and plant responses to elevated CO_2: New Phytologist, v. 167, n. 3, p. 859–868, doi:10.1111/j.1469-8137.2005.01458.x.

Arthur, M. A., and Fahey, T. J., 1993, Controls on soil solution chemistry in a subalpine forest in north-central Colorado: Soil Science Society of America Journal, v. 57, n. 4, p. 1122–1122, doi:10.2136/sssaj1993.03615995005700040040x.

Arvieu, J.-C., Leprince, F., and Plassard, C., 2003, Release of oxalate and protons by ectomycorrhizal fungi in response to P-deficiency and calcium carbonate in nutrient solution: Annals of Forest Science, v. 60, p. 815–821, doi:10.1051/forest:2003076.

Ashton, P. S., 2003, Dipterocarpaceae, *in* Kubitzki, K., and Bayer, C., editors, Flowering plants, dicotyledons: Malvales, Capparales, and non-betalain Caryophyllales: New York, Springer-Verlag, p. 182–197.

Augusto, L., Ranger, J., Binkley, D., and Rothe, A., 2002, Impact of several common tree species of European

temperate forests on soil fertility: Annals of Forest Science, v. 59, n. 3, p. 233–253, doi:10.1051/forest:2002020.
Banwart, S. A., Berg, A., and Beerling, D. J., 2009, Process-based modeling of silicate mineral weathering responses to increasing atmospheric CO_2 and climate change: Global Biogeochemical Cycles, v. 23, p. GB4013, doi:10.1029/2008GB003243.
Bayer, C., 2003, Sarcolaenaceae, *in* Kubitzki, K., and Bayer, C., editors, Flowering plants, dicotyledons: Malvales, Capparales, and non-betalain Caryophyllales: New York, Springer-Verlag, p. 345–352.
Beerling, D. J., and Woodward, F. I., 2001, Vegetation and the terrestrial carbon cycle: modelling the first 400 million years: Cambridge, Cambridge University Press, 405 p.
Berg, A., and Banwart, S. A., 2000, Carbon dioxide mediated dissolution of Ca-feldspar: implications for silicate weathering: Chemical Geology, v. 163, n. 1–4, p. 25–42, doi:10.1016/S0009-2541(99)00132-1.
Bergman, N., Lenton, T., and Watson, A. J., 2004, COPSE: A new model of biogeochemical cycling over Phanerozoic time: American Journal of Science, v. 304, p. 397–437, doi:10.2475/ajs.304.5.397.
Berner, E. K., Berner, R. A., and Moulton, K. L., 2003, Plants and mineral weathering: past and present, *in* Holland, H. D., and Turekian, K. K., editors, Surface and Ground Water, Weathering, and Soils: Elsevier, Treatise on Geochemistry, v. 5, p. 169–188, doi:10.1016/B0-08-043751-6/05175-6.
Berner, R., 1991, A model for atmospheric CO_2 over Phanerozoic time, American Journal of Science, v. 291, p. 339–376, doi:10.2475/ajs.291.4.339.
——— 1994, GEOCARB II; a revised model of atmospheric CO_2 over Phanerozoic time: American Journal of Science, v. 294, p. 56–91, doi:10.2475/ajs.294.1.56.
——— 2004, The Phanerozoic Carbon Cycle: CO_2 and O_2: Oxford, Oxford University Press, 150 p.
——— 2006a, GEOCARBSULF: A combined model for Phanerozoic atmospheric O_2 and CO_2: Geochimica et Cosmochimica Acta, v. 70, n. 23, p. 5653–5664, doi:10.1016/j.gca.2005.11.032.
——— 2006b, Inclusion of the Weathering of Volcanic Rocks in the GEOCARBSULF Model: American Journal of Science, v. 306, p. 295–302, doi:10.2475/05.2006.01.
——— 2008, Addendum to "Inclusion of the Weathering of Volcanic Rocks in the GEOCARBSULF Model": American Journal of Science, v. 308, p. 100–103, doi:10.2475/01.2008.04.
Berner, R. A., and Kothavala, Z., 2001, Geocarb III: A Revised Model of Atmospheric CO_2 over Phanerozoic Time: American Journal of Science, v. 301, p. 182–204, doi:10.2475/ajs.301.2.182.
Berner, R., and Maasch, K., 1996, Chemical weathering and controls on atmospheric O_2 and CO_2: Fundamental principles were enunciated by JJ Ebelmen in 1845: Geochimica et Cosmochimica Acta, v. 60, p. 1633–1637, doi:10.1016/0016-7037(96)00104-4.
Blasco, F., Bellan, M., and Aizpuru, M., 1996, A vegetation map of tropical continental Asia at scale 1: 5 million: Journal of Vegetation Science, v. 7, p. 623–634.
Bluth, G. J. S., and Kump, L. R., 1991, Phanerozoic paleogeology: American Journal of Science, v. 291, p. 284–308, doi:10.2475/ajs.291.3.284.
Boerner, R. E. J., 1982, Fire and nutrient cycling in temperate ecosystems: BioScience, v. 32, n. 3, p. 187–192, doi:10.2307/1308941.
Bolan, N. S., and Hedley, M. J., 2003, Role of carbon, nitrogen and sulphur cycles in soil acidification, *in* Rengel, Z., editor, Handbook of Soil Acidity: New York, Marcel Dekker, Inc., p. 29–56.
Boyce, C. K., Brodribb, T. J., Feild, T. S., and Zwieniecki, M. A., 2009, Angiosperm leaf vein evolution was physiologically and environmentally transformative: Proceedings of the Royal Society B: Biological Sciences, v. 276, p. 1771–1776, doi:10.1098/rspb.2008.1919.
Brantley, S., 2008, Kinetics of Mineral Dissolution, *in* Brantley, S. L., Kubicki, J. D., and White, A. F., editors, Kinetics of Water-Rock Interaction: New York, Springer Science+Business Media, LLC, p. 151–210.
Brownlee, C., Duddridge, J. A., Malibari, A., and Read, D. J., 1983, The structure and function of mycelial systems of ectoymcorrhizal roots with special reference to their role in forming inter-plant connections and providing pathways for assimilate and water transport: Plant and Soil, v. 71, p. 433–443, doi:10.1007/BF02182684.
Brundrett, M. C., 2002, Coevolution of roots and mycorrhizas of land plants: New Phytologist, v. 154, p. 275–304, doi:10.1046/j.1469-8137.2002.00397.x.
Casarin, V., Plassard, C., Souche, G., and Arvieu, J.-C., 2003, Quantification of oxalate ions and protons released by ectomycorrhizal fungi in rhizosphere soil: Agronomie, v. 23, p. 461–469, doi:10.1051/agro:2003020.
Cerling, T., 1991, Carbon dioxide in the atmosphere: evidence from Cenozoic and Mesozoic paleosols: American Journal of Science, v. 291, p. 377–400, doi:10.2475/ajs.291.4.377.
Crane, P. R., and Lidgard, S., 1989, Angiosperm diversification and paleolatitudinal gradients in Cretaceous floristic diversity: Science, v. 246, p. 675–678, doi:10.1126/science.246.4930.675.
Cromack, K., Sollins, P., Todd, R., Fogel, R., Todd, A., Fender, W., Crossley, M., and Crossley, D., 1977, The role of oxalic acid and bicarbonate in calcium cycling by fungi and bacteria: some possible implications for soil animals: Ecological Bulletins, v. 25, p. 246–252.
Cromack, K., Jr., Sollins, P., Graustein, W. C., Speidel, K., Todd, A. W., Spycher, G., Li, C. Y., and Todd, R. L., 1979, Calcium oxalate accumulation and soil weathering in mats of the hypogeous fungus *Hysterangium crassum:* Soil Biology and Biochemistry, v. 11, n. 5, p. 463–468, doi:10.1016/0038-0717(79)90003-8.
Dessert, C., Dupré, B., Gaillardet, J, François, L. M., and Allègre, C. J., 2003, Basalt weathering laws and the impact of basalt weathering on the global carbon cycle: Chemical Geology, v. 202, n. 3–4, p. 257–273, doi:10.1016/j.chemgeo.2002.10.001.
Douglas, J. G., and Williams, G. E., 1982, Southern polar forests: the Early Cretaceous floras of Victoria and their palaeoclimatic significance: Palaeogeography, Palaeoclimatology, Palaeoecology, v. 39, n. 3–4, p. 171–185, doi:10.1016/0031-0182(82)90021-9.
Drever, J. I., and Zobrist, J., 1992, Chemical weathering of silicate rocks as a function of elevation in the

southern Swiss Alps: Geochimica et Cosmochimica Acta, v. 56, n. 8, p. 3209–3216, doi:10.1016/0016-7037(92)90298-W.

Ducousso, M., Béna, G., Bourgeois, C., Buyck, B., Eyssartier, G., Vincelette, M., Rabevohitra, R., Randrihasipara, L., Dreyfus, B., and Prin, Y., 2004, The last common ancestor of Sarcolaenaceae and Asian dipterocarp trees was ectomycorrhizal before the India-Madagascar separation, about 88 million years ago: Molecular Ecology, v. 13, n. 1, p. 231–236, doi:10.1046/j.1365-294X.2003.02032.x.

Duddridge, J. A., Malibari, A., and Read, D. J., 1980, Structure and function of mycorrhizal rhizomorphs with special reference to their role in water transport: Nature, v. 287, p. 834–836, doi:10.1038/287834a0.

Ebelmen, J., 1845, Sur les produits de la decomposition des especes minerales de la famille des silicates: Annales des Mines, v. 7, p. 3–66.

Ekart, D. D., Cerling, T. E., Montanez, I. P., and Tabor, N. J., 1999, A 400 million year carbon isotope record of pedogenic carbonate: implications for paleoatmospheric carbon dioxide: American Journal of Science, v. 299, p. 805–827, doi:10.2475/ajs.299.10.805.

Falcon-Lang, H., 2000, A method to distinguish between woods produced by evergreen and deciduous coniferopsids on the basis of growth ring anatomy: a new palaeoecological tool: Palaeontology, v. 43, p. 785–793, doi:10.1111/1475-4983.00149.

Gadd, G. M., 2007, Geomycology: biogeochemical transformations of rocks, minerals, metals and radionuclides by fungi, bioweathering and bioremediation: Mycological Research, v. 111, n. 1, p. 3–49, doi:10.1016/j.mycres.2006.12.001.

Gaillardet, J., Dupré, B., Louvat, P., and Allegre, C., 1999, Global silicate weathering and CO_2 consumption rates deduced from the chemistry of large rivers: Chemical Geology, v. 159, p. 3–30, doi:10.1016/S0009-2541(99)00031-5.

Gibbs, M. T., and Kump, L. R., 1994, Global chemical erosion during the last glacial maximum and the present: Sensitivity to changes in lithology and hydrology: Paleoceanography, v. 9, n. 4, p. 529–543, doi:10.1029/94PA01009.

Gibbs, M. T., Bluth, J. S. G., Fawcett, P. J., and Kump, L. R., 1999, Global chemical erosion over the last 250 my; variations dueto changes in paleogeography, paleoclimate, and paleogeology: American Journal of Science, v. 299, p. 611–651, doi:10.2475/ajs.299.7-9.611.

Goddéris, Y., Donnadieu, Y., Tombozafy, M., and Dessert, C., 2008, Shield effect on continental weathering: implication for climatic evolution of the earth at the geological timescale: Geoderma, v. 145, n. 3–4, 439–448, doi:10.1016/j.geoderma.2008.01.020.

Griffiths, R. P., Baham, J. E., and Caldwell, B. A., 1994, Soil solution chemistry of ectomycorrhizal mats in forest soil: Soil Biology and Biochemistry, v. 26, n. 3, p. 331–337, doi:10.1016/0038-0717(94)90282-8.

Hardie, L. A., 1996, Secular variation in seawater chemistry: An explanation for the coupled secular variation in the mineralogies of marine limestones and potash evaporites over the past 600 m.y.: Geology, v. 24, n. 3, p. 279–283, doi:10.1130/0091-7613(1996)024⟨0279:SVISCA⟩2.3.CO;2.

Hartmann, J., Jansen, N., Dürr, H. H., Kempe, S., and Köhler, P., 2009, Global CO_2-consumption by chemical weathering: What is the contribution of highly active weathering regions?: Global and Planetary Change, v. 69, n. 4, p. 185–194, doi:10.1016/j.gloplacha.2009.07.007.

Hinsinger, P., Gobran, G. R., Gregory, P. J., and Wenzel, W. W., 2005, Rhizosphere geometry and heterogeneity arising from root-mediated physical and chemical processes: New Phytologist, v. 168, n. 2, p. 293–303, doi:10.1111/j.1469-8137.2005.01512.x.

Hodson, M. E., and Langan, S. J., 1999, The influence of soil age on calculated mineral weathering rates: Applied Geochemistry, v. 14, n. 3, p. 387–394, doi:10.1016/S0883-2927(98)00052-3.

Hodson, M. E., Langan, S. J., Kennedy, F. M., and Bain, D. C., 1998, Variation in soil surface area in a chronosequence of soils from Glen Feshie, Scotland and its implications for mineral weathering rate calculations: Geoderma, v. 85, n. 1, p. 1–18, doi:10.1016/S0016-7061(98)00013-5.

Hoffland, E., Kuyper, T. W., Wallander, H., Plassard, C., Gorbushina, A. A., Haselwandter, K., Holmström, S., Landeweert, R., Lundström, U. S., Rosling, A., Sen, R., Smits, M. M., van Hees, P. A. W., and van Breemen, N., 2004, The role of fungi in weathering: Frontiers in Ecology and the Environment, v. 2, p. 258–264, doi:10.1890/1540-9295(2004)002[0258:TROFIW]2.0.CO;2.

Hüttl, R. F., and Schaaf, W., 1995, Nutrient supply of forest soils in relation to management and site history: Plant and Soil, v. 168–169, n. 1, p. 31–41, doi:10.1007/BF00029311.

Ingleby, K., Diagne, O., Deans, J. D., Lindley, D. K., Neyra, M., and Ducousso, M., 1997, Distribution of roots, arbuscular mycorrhizal colonisation and spores around fast-growing tree species in Senegal: Forest Ecology and Management, v. 90, n. 1, p. 19–27, doi:10.1016/S0378-1127(96)03875-3.

Jackson, R., Mooney, H. A., and Schulze, E.-D., 1997, A global budget for fine root biomass, surface area, and nutrient contents: Proceedings of the National Academy of Sciences, v. 94, p. 7362–7366, doi:10.1073/pnas.94.14.7362.

Jobbágy, E. G., and Jackson, R. B., 2003, Patterns and mechanisms of soil acidification in the conversion of grasslands to forests: Biogeochemistry, v. 64, n. 2, p. 205–229, doi:10.1023/A:1024985629259.

Johansson, E. M., Fransson, P. M. A., Finlay, R. D., and van Hees, P. A. W., 2008, Quantitative analysis of root and ectomycorrhizal exudates as a response to Pb, Cd and As stress: Plant and Soil, v. 313, n. 1–2, p. 39–54, doi:10.1007/s11104-008-9678-1.

Jones, D. L., and Darrah, P. R., 1995, Influx and efflux of organic acids across the soil-root interface of *Zea mays* L. and its implications in rhizosphere C flow: Plant and Soil, v. 173, n. 1, p. 103–109, doi:10.1007/BF00155523.

Kim, T. K., and Silk, W. K., 1999, A mathematical model for pH patterns in the rhizospheres of growth zones: Plant, Cell and Environment, v. 22, n. 12, p. 1527–1538, doi:10.1046/j.1365-3040.1999.00512.x.

Klironomos, J. N., Rillig, M. C., Allen, M. F., Zak, D. R., Kubiske, M., and Pregitzer, K. S., 1997, Soil fungal-arthropod responses to *Populus tremuloides* grown under enriched atmospheric CO_2 under field conditions: Global Change Biology, v. 3, n. 6, p. 473–478, doi:10.1046/j.1365-2486.1997.00085.x.

Knoepp, J. D., and Swank, W. T., 1994, Long-term soil chemistry changes in aggrading forest ecosystems: Soil Science Society of America Journal, v. 58, n. 2, p. 325–331, doi:10.2136/sssaj1994.03615995005800020010x.

Knoll, M. A., and James, W. C., 1987, Effect of the advent and diversification of vascular land plants on mineral weathering through geologic time: Geology, v. 15, n. 12, p. 1099–1102, doi:10.1130/0091-7613(1987)15⟨1099:EOTAAD⟩2.0.CO;2.

Landeweert, R., Hoffland, E., Finlay, R. D., Kuyper, T. W., and van Breemen, N., 2001, Linking plants to rocks: ectomycorrhizal fungi mobilize nutrients from minerals: Trends in Ecology and Evolution, v. 16, n. 5, p. 248–254, doi:10.1016/S0169-5347(01)02122-X.

Leake, J. R., Johnson, D. J., Donnelly, D., Muckle, G., Boddy, L., and Read, D. J., 2004, Networks of power and influence: the role of mycorrhizal mycelium in controlling plant communities and agroecosystem functioning: Canadian Journal of Botany, v. 82, n. 8, p. 1016–1045, doi:10.1139/b04-060.

Leake, J. R., Duran, A. L., Hardy, K. E., Johnson, I., Beerling, D. J., Banwart, S. A., and Smits, M. M., 2008, Biological weathering in soil: the role of symbiotic root-associated fungi biosensing minerals and directing photosynthate-energy into grain-scale mineral weathering: Mineralogical Magazine, v. 72, p. 85–89.

Li, X.-L., George, E., and Marschner, H., 1991, Extension of the phosphorus depletion zone in VA-mycorrhizal white clover in a calcareous soil: Plant and Soil, v. 136, n. 1, p. 41–48, doi:10.1007/BF02465218.

Lidgard, S., and Crane, P., 1988, Quantitative analyses of the early angiosperm: Radiation: Nature, v. 331, p. 344–346, doi:10.1038/331344a0.

——— 1990, Angiosperm diversification and Cretaceous floristic trends: a comparison of palynofloras and leaf macrofloras: Paleobiology, v. 16, n. 1, p. 77–93.

Malhi, Y., Baldocchi, D. D., and Jarvis, P. G., 1999, The carbon balance of tropical, temperate and boreal forests: Plant, Cell and Environment, v. 22, n. 6, p. 715–740, doi:10.1046/j.1365-3040.1999.00453.x.

Malmer, A., 1996, Hydrological effects and nutrient losses of forest plantation establishment on tropical rainforest land in Sabah, Malaysia: Journal of Hydrology, v. 174, n. 1–2, p. 129–148, doi:10.1016/0022-1694(95)02757-2.

Marschner, H., 1995, Mineral nutrition of higher plants: London, Academic Press, 889 p.

Marschner, H., Häussling, M., and George, E., 1991, Ammonium and nitrate uptake rates and rhizosphere pH in non-mycorrhizal roots of Norway spruce *Picea abies* (L.) Karst: Trees—Structure and Function, v. 5, p. 14–21.

Martino, E., Perotto, S., Parsons, R., and Gadd, G. M., 2003, Solubilization of insoluble inorganic zinc compounds by ericoid mycorrhizal fungi derived from heavy metal polluted sites: Soil Biology and Biochemistry, v. 35, n. 1, p. 133–141, doi:10.1016/S0038-0717(02)00247-X.

Miller, H. G., 1995, The influence of stand development on nutrient demand, growth and allocation: Plant and Soil, v. 168–169, p. 225–232, doi:10.1007/BF00029332.

Moulton, K. L., West, J., and Berner, R. A., 2000, Solute flux and mineral mass balance approaches to the quantification of plant effects on silicate weathering: American Journal of Science, v. 300, p. 539–570, doi:10.2475/ajs.300.7.539.

Moyersoen, B., 2006, *Pakaraimaea dipterocarpacea* is ectomycorrhizal, indicating an ancient Gondwanaland origin for the ectomycorrhizal habit in Dipterocarpaceae: New Phytologist, v. 172, n. 4, p. 753–762, doi:10.1111/j.1469-8137.2006.01860.x.

Navarre-Sitchler, A., and Brantley, S., 2007, Basalt weathering across scales: Earth and Planetary Science Letters, v. 261, n. 1–2, p. 321–334, doi:10.1016/j.epsl.2007.07.010.

Neaman, A., Chorover, J., and Brantley, S. L., 2006, Effects of organic ligands on granite dissolution in batch experiments at pH 6: American Journal of Science, v. 306, p. 451–473, doi:10.2475/06.2006.03.

Nilsson, S. I., Miller, H. G., and Miller, J. D., 1982, Forest growth as a possible cause of soil and water acidification: an examination of the concepts: Oikos, v. 39, p. 40–49, doi:10.2307/3544529.

Nilsson, S., Coetzee, J., and Grafström, E., 1996, On the origin of the Sarcolaenaceae with reference to pollen morphological evidence: Grana, v. 35, n. 6, p. 321–334, doi:10.1080/00173139609429091.

Nockolds, S. R., 1954, Average chemical compositions of some igneous rocks: Geological Society of America Bulletin, v. 65, n. 10, p. 1007–1032, doi:10.1130/0016-7606(1954)65[1007:ACCOSI]2.0.CO;2.

Norby, R. J., O'Neill, E. G., and Luxmoore, R. J., 1986, Effects of atmospheric CO_2 enrichment on the growth and mineral nutrition of *Quercus alba* seedlings in nutrient-poor soil: Plant Physiology, v. 82, p. 83–89, doi:10.1104/pp.82.1.83.

Norby, R. J., Hanson, P. J., O'Neill, E. G., Tschaplinski, T. J., Weltzin, J. F., Hansen, R. A., Cheng, W., Wullschleger, S. D., Gunderson, C. A., Edwards, N. T., and Johnson, D. W., 2002, Net primary productivity of a CO_2-enriched deciduous forest and the implications for carbon storage: Ecological Applications, v. 12, n. 5, p. 1261–1266, doi:10.1890/1051-0761(2002)012[1261:NPPOAC]2.0.CO;2.

Norby, R. J., Ledford, J., Reilly, C. D., Miller, N. E., and O'Neill, E. G., 2004, Fine-root production dominates response of a deciduous forest to atmospheric CO_2 enrichment: Proceedings of the National Academy of Sciences of the United States of America, v. 101, n. 26, p. 9689–9693, doi:10.1073/pnas.0403491101.

Norby, R. J., DeLucia, E. H., Gielen, B., Calfapietra, C., Giardina, C. P., King, J. S., Ledford, J., McCarthy, H. R., Moore, D. J. P., Ceulemans, R., de Angelis, P., Finzi, A. C., Karnosky, D. F., Kubiske, M. E., Lukac, M., Pregitzer, K. s., Scarascia-Mignozza, G. E., Schlesinger, W. H., and Oren, R. 2005, Forest response to elevated CO_2 is conserved across a broad range of productivity: Proceedings of the National Academy of Sciences of the United States of American, v. 102, n. 50, p. 18052–18056, doi:10.1073/pnas.0509478102.

Nye, P., 1981, Changes of pH across the rhizosphere induced by roots: Plant and Soil, v. 61, n. 1–2, p. 7–26, doi:10.1007/BF02277359.

Otto-Bliesner, B. L., 1995, Continental drift, runoff, and weathering feedbacks: implications from climate

model experiments: Journal of Geophysical Research, v. 100, n. D6, p. 11537–11548, doi:10.1029/95JD00591.

Pagani, M., Caldeira, K., Berner, R., and Beerling, D. J., 2009, The role of terrestrial plants in limiting atmospheric CO_2 decline over the past 24 million years: Nature, v. 460, p. 85–89, doi:10.1038/nature08133.

Palandri, J., and Kharaka, Y., 2004, A compilation of rate parameters of water-mineral interaction kinetics for application to geochemical modeling: Menlo Park, California, Geological Survey, US Geological Survey Open File Report 2004-1068, 70 p.

Pregitzer, K. S., DeForest, J. L., Burton, A. J., Allen, M. F., Ruess, R. W., and Hendrick, R. L., 2002, Fine root architecture of nine North American trees: Ecological Monographs, v. 72, n. 2, p. 293–309, doi:10.1890/0012-9615(2002)072[0293:FRAONN]2.0.CO;2.

Querejeta, J. I., Egerton-Warburton, L. M., and Allen, M. F., 2003, Direct nocturnal water transfer from oaks to their mycorrhizal symbionts during severe soil drying: Ecophysiology, v. 134, p. 55–64, doi:10.1007/s00442-002-1078-2.

Radersma, S., and Grierson, P. F., 2004, Phosphorus mobilization in agroforestry: organic anions, phosphatase activity and phosphorus fractions in the rhizosphere: Plant and Soil, v. 259, n. 1–2, p. 209–219, doi:10.1023/B:PLSO.0000020970.40167.40.

Read, D. J., 1991, Mycorrhizas in ecosystems: Experientia, v. 47, p. 376–391, doi:10.1007/BF01972080.

Rees, P. McA., Gibbs, M. T., Ziegler, A. M., Kutzbach, J. E., and Behling, P. J., 1999, Permian climates: Evaluating model predictions using global paleobotanical data: Geology, v. 27, n. 10, p. 891–894, doi:10.1130/0091-7613(1999)027⟨0891:PCEMPU⟩2.3.CO;2.

Robinson, D., 1996, Resource capture by localized root proliferation: Why do plants bother?: Annals of Botany, v. 77, n. 2, p. 179–185, doi:10.1006/anbo.1996.0020.

Roelandt, C., Goddéris, Y., Bonnet, M.-P., and Sondag, F., 2010, Coupled modeling of biospheric and chemical weathering processes at the continental scale: Global Biogeochemical Cycles, v. 24, p. GB2004, doi:10.1029/2008GB003420.

Rosling, A., Lindahl, B. D., Taylor, A. F. S., and Finlay, R. D., 2004, Mycelial growth and substrate acidification of ectomycorrhizal fungi in response to different minerals: FEMS microbiology ecology, v. 47, p. 31–37, doi:10.1016/S0168-6496(03)00222-8.

Rust, J., Singh, H., Rana, R. S., McCann, T., Singh, L., Anderson, K., Sarkar, N., Nascimbene, P. C., Stebner, F., Thomas, J. C., Kraemer, M. S., Williams, C. J., Engel, M. S., Sahni, A., and Grimaldi, D., 2010, Biogeographic and evolutionary implications of a diverse paleobiota in amber from the early Eocene of India: Proceedings of the National Academy of Sciences, v. 107, n. 43, p. 18360–18365, doi:10.1073/pnas.1007407107.

Ryan, P. R., Delhaize, E., and Jones, D. L., 2001, Function and mechanism of organic anion exudation from plant roots: Annual Review of Plant Physiology and Plant Molecular Biology, v. 52, p. 527–560, doi:10.1146/annurev.arplant.52.1.527.

Saugier, B., Roy, J., and Mooney, H. A., 2001, Estimations of global terrestrial productivity: converging toward a single number, *in* Roy, J., Saugier, B., and Mooney, H. A., editors, Terrestrial global productivity: San Diego, Academic Press, p. 543–557.

Schnoor, J., and Stumm, W., 1986, The role of chemical weathering in the neutralization of acidic deposition: Aquatic Sciences—Research Across Boundaries, v. 48, n. 2, p. 171–195, doi:10.1007/BF02560197.

Smith, S. E., and Read, D. J., 2008, Mycorrhizal symbiosis: London, Academic Press, 787 p.

Spicer, R. A., and Chapman, J. L., 1990, Climate change and the evolution of high-latitude terrestrial vegetation and floras: Trends in Ecology and Evolution, v. 5, n. 9, p. 279–284, doi:10.1016/0169-5347(90)90081-N.

Spicer, R. A, and Parrish, J. T., 1986, Paleobotanical evidence for cool north polar climates in middle Cretaceous(Albian-Cenomanian) time: Geology, v. 14, n. 8, p. 703–706, doi:10.1130/0091-7613(1986)14⟨703:PEFCNP⟩2.0.CO;2.

Stallard, R. F., 1995, Tectonic, environmental, and human aspects of weathering and erosion: A global review using a steady-state perspective: Annual Review of Earth and Planetary Sciences, v. 23, p. 11–39, doi:10.1146/annurev.ea.23.050195.000303.

Stillings, L. L., Drever, J. I., Brantley, S. L., Sun, Y., and Oxburgh, R., 1996, Rates of feldspar dissolution at pH 3–7 with 0–8 mM oxalic acid: Chemical Geology, v. 132, n. 1–4, p. 79–89, doi:10.1016/S0009-2541(96)00043-5.

Stumm, W., and Morgan, J., 1996, Aquatic chemistry: chemical equilibria and rates in natural waters: New York, New York, John Wiley and Sons, 1040 p.

Sun, Y.-P., Unestam, T., Lucas, S. D., Johanson, K. J., Kenne, L., and Finlay, R., 1999, Exudation-reabsorption in a mycorrhizal fungus, the dynamic interface for interatction with soil and soil microorganisms: Mycorrhiza, v. 9, n. 3, p. 137–144, doi:10.1007/s005720050298.

Taylor, L. L., Leake, J. J., Quirk, J., Hardy, K., Banwart, S. A., and Beerling, D. J., 2009, Biological weathering and the long-term carbon cycle: integrating mycorrhizal evolution and function into the current paradigm: Geobiology, v. 7, n. 2, p. 171–191, doi:10.1111/j.1472-4669.2009.00194.x.

Thelin, G., Sverdrup, H., Holmqvist, J., Rosengren, U., and Linden, M., 2002, Sustainability in spruce and mixed-species stands: Assessing nutrient sustainability for single stands at Jämjö, *in* Sverdrup, H., and Stjernquist, I., editors, Developing Principles and Models for Sustainable Forestry in Sweden: Dordrecht, Kluwer Academic Publishers, p. 337–354.

Unestam, T., 1991, Water repellency, mat formation, and leaf-stimulated growth of some ectomycorrhizal fungi: Mycorrhiza, v. 1, n. 1, p. 13–20, doi:10.1007/BF00205897.

Unestam, T., and Sun, Y.-P., 1995, Extramatrical structures of hydrophobic and hydrophilic ectomycorrhizal fungi: Mycorrhiza, v. 5, n. 5, p. 301–311, doi:10.1007/BF00207402.

Urey, H., 1952, The planets, their origin and development: New Haven, Connecticut, Yale University Press, 247 p.

Vakhrameev, V. A., and Hughes, N. F., 1991, Jurassic and Cretaceous floras and climates of the Earth: Cambridge, United Kingdom, Cambridge University Press, 340 p.

van Hees, P. A. W., Jones, D. L., Finlay, R., Godbold, D. L., and Lundström, U. S., 2005a, The carbon we do not see—the impact of low molecular weight compounds on carbon dynamics and respiration in forest soils: a review: Soil Biology and Biochemistry, v. 37, n. 1, p. 1–13, doi:10.1016/j.soilbio.2004.06.010.

van Hees, P. A. W., Jones, D. L., Jentschke, G., and Godbold, D. L., 2005b, Organic acid concentrations in soil solution: effects of young coniferous trees and ectomycorrhizal fungi: Soil Biology and Biochemistry, v. 37, n. 4, p. 771–776, doi:10.1016/j.soilbio.2004.10.009.

van Hees, P. A. W., Rosling, A., Essen, S., Godbold, D. L., Jones, D. L., and Finlay, R. D., 2006, Oxalate and ferricrocin exudation by the extramatrical mycelium of an ectomycorrhizal fungus in symbiosis with *Pinus sylvestris:* New Phytologist, v. 169, n. 2, p. 367–378, doi:10.1111/j.1469-8137.2005.01600.x.

Volk, T., 1987, Feedbacks between weathering and atmospheric CO_2 over the last 100 million years: American Journal of Science, v. 287, p. 763–779, doi:10.2475/ajs.287.8.763.

——— 1989, Rise of angiosperms as a factor in long-term climatic cooling: Geology, v. 17, n. 2, p. 107–110, doi:10.1130/0091-7613(1989)017⟨0107:ROAAAF⟩2.3.CO;2.

Wallander, H., Göransson, H., and Rosengren, U., 2004, Production, standing biomass and natural abundance of ^{15}N and ^{13}C in ectomycorrhizal mycelia collected at different soil depths in two forest types: Oecologia, v. 139, n. 1, p. 89–97, doi:10.1007/s00442-003-1477-z.

Wang, B., and Qiu, Y. L., 2006, Phylogenetic distribution and evolution of mycorrhizas in land plants: Mycorrhiza, v. 16, n. 5, p. 299–363, doi:10.1007/s00572-005-0033-6.

White, A. F., and Brantley, S. L., 2003, The effect of time on the weathering of silicate minerals: why do weathering rates differ in the laboratory and field?: Chemical Geology, v. 202, n. 3–4, p. 479–506, doi:10.1016/j.chemgeo.2003.03.001.

White, A. F., Blum, A. E., Schulz, M. S., Bullen, T. D., Harden, J. W., and Peterson, M. L., 1996, Chemical weathering rates of a soil chronosequence on granitic alluvium: I. Quantification of mineralogical and surface area changes and calculation of primary silicate reaction rates: Geochimica et Cosmochimica Acta, v. 60, n. 14, p. 2533–2550, doi:10.1016/0016-7037(96)00106-8.

White, A. F., Schulz, M. S., Vivit, D. V., Blum, A. E., Stonestrom, D. A., and Harden, J. W., 2005, Chemical weathering rates of a soil chronosequence on granitic alluvium: III. Hydrochemical evolution and contemporary solute fluxes and rates: Geochimica et Cosmochimica Acta, v. 69, n. 8, p. 1975–1996, doi:10.1016/j.gca.2004.10.003.

Wilson, M. J., 2006, Factors of soil formation: parent material. as exemplified by a comparison of granitic and basaltic soils., *in* Certini, G., Scalenghe, R., and Ugolini, F. C., editors, Soils: Basic Concepts and Future Challenges: Cambridge, United Kingdom, Cambridge University Press, p. 113–130, http://dx.doi.org/10.1017/CBO9780511535802.010.

Wing, S. L., and Boucher, L. D., 1998, Ecological aspects of the Cretaceous flowering plant radiation: Annual Review of Earth and Planetary Science, v. 26, p. 379–421, doi:10.1146/annurev.earth.26.1.379.

Wösten, H. A., Schuren, F. H., and Wessels, J. G., 1994, Interfacial self-assembly of a hydrophobin into an amphipathic protein membrane mediates fungal attachment to hydrophobic surfaces: The EMBO Journal, v. 13, p. 5848–5854.

Zhang, H., and Bloom, P. R., 1999, Dissolution Kinetics of Hornblende in Organic Acid Solutions: Soil Science Society of America Journal, v. 63, n. 4, p. 815–822, doi:10.2136/sssaj1999.634815x.